Waterstof in Dwingeloo

“Waterstof in je achtertuin”
14 maart 2026, Dwingeloo

Thomas Telkamp

Opening door Ed Dusschoten

Waarom zijn we hier?

- Karl Jansky van Bell Telephone Laboratories ontdekte bij toeval (1932) dat:
  - Er radiogolven uit het heelal komen.
  - Het signaal zich elke 23 uur en 56 minuten herhaalt.

- De Leidse astronoom Jan Oort:
  - Ziet mogelijke correlatie radiogolven en Melkweg
  - Wil de Melkweg in kaart brengen.
  - 1944: Opdracht aan student Henk van de Hulst: Hebben radiogolven betekenis voor de astronomie?

- Oort/ Hendrik van de Hulst tonen aan dat:
  - Waterstofatomen radiogolven uitzenden op een golflengte van 21,105 centimeter (de "21-cm waterstof spectraallijn met dus een frequentie van 1420,4 MHz")
  - Deze radio golven op specifieke plaatsen in het heelal zitten, zoals het Melkwegstelsel.

Waarom zijn we hier? (2)

Eerste waterstof waarnemingen werden gedaan op de PTT locatie Radio Kootwijk door Christiaan Alexander (Lex) Muller.

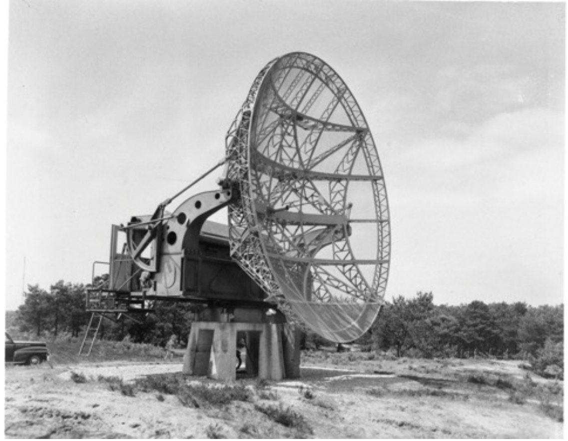

De waarneming werd uitgevoerd met een omgebouwde Duits Radar station “Der Würzburg-Riese”. Deze waren massaal na de oorlog door de Duitsers achter gelaten.

Er was veel storing in de omgeving van Kootwijk en de spiegel was klein.

Een nieuwe “stillere” (= minder storing) locatie werd gezocht en gevonden op het Dwingeler veld. Er werd gekeken naar grotere nieuwbouw.

In 1953 wordt begonnen met de bouw.

Daarom zijn we hier!

- In 1956 opent Ko... ...liana de Dwingeloo Radiotelescoop... Dan op dat mo... ...ld!
- Het startmo... Melkweg werd in...

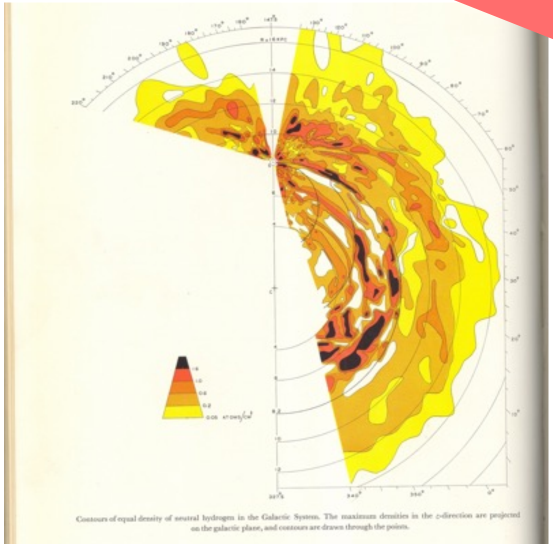

70 jaar later hebben de Camras vrijwilligers
Jan van Muijlwijk,
Gerard Boons,
Tammo-Jan Dijkema,
Thomas Telkamp
het seminar 'Waterstof in je achter tuin' georganiseerd!

- Te gast bij ASTRON
- Geen consumpties in het auditorium
- Microfoons gebruiken
- Badge graag inleveren aan eind van de dag
- Presentaties online via CAMRAS website
  - https://data.camras.nl/seminar-2026/

Waterstof in je achtertuin

CAMRAS seminar zaterdag 14 maart 2026

9:30 – 10:00 **Inloop, koffie en thee**
Centrale hal

10:00 – 10:15 **Opening en welkom**
Ed Dusschoten, CAMRAS
Van de Hulst Auditorium

10:15 – 10:45 **Waterstof in Dwingeloo**
Thomas Telkamp (CAMRAS)

10:45 – 11:15 **Blik op de Melkweg: astrofysische metingen met een ‘cantenna’**
Michiel Brentjens (ASTRON / Universiteit Leiden)

11:15 – 11:45 **Pauze**
Centrale hal

11:45 – 12:15 **Metingen aan de Melkweg met een 1,5-meter schoteltje**
Frans de Jong (CAMRAS)

12:15 – 12:45 **Sterrenstelsels op 21cm**
Eduard Mol

12:45 – 13:30 **Lunch**
Kantine

13:30 – 15:00 **Demonstraties en buitenprogramma**
- Demonstraties van meegebrachte ontvangers
- Doorlopend waterstofmetingen in de Dwingeloo telescoop
- First light van 2.5m-schotel CAMRAS
- Virtual reality visualisatie van all-sky waterstofmetingen
- Posterpresentaties

15:00 – 15:30 **Professionele HI-astronomie in Dwingeloo, Westerbork en daarna**
Tom Oosterloo (ASTRON / Universiteit Groningen)
Van de Hulst Auditorium

15:30 – 17:00 **Borrel**
Centrale hal

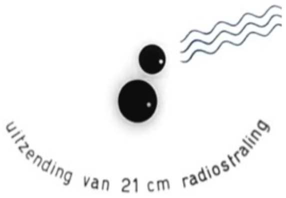


Hoofdingang
⑤
Oude Hoogeveensedijk
Oude Hoogeveensedijk
Davidshoeve
④
③
②
①
Middagprogramma
1. 25m-schotel
2. 2,5m-schotel
3. Antennes buiten
4. Antennes binnen
5. Posters, software
en VR-datavisualisatie

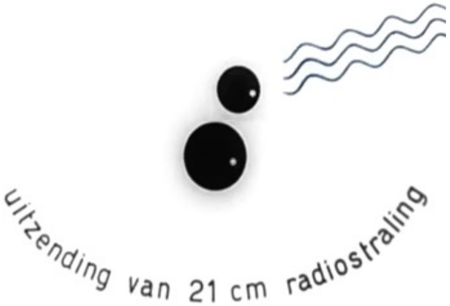

2026

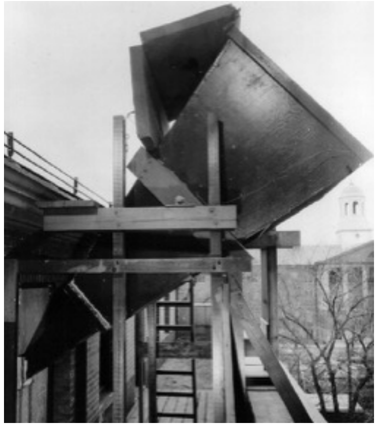

75 jaar

70 jaar

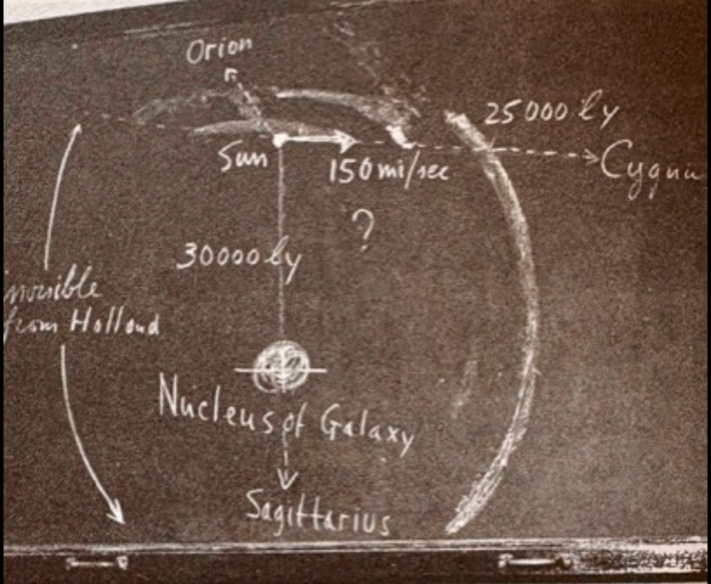
Orion
25000 ly
Sun
150 mi/sec
Cygnu
?
30000 ly
nvisible
from Holland
Nucleus of Galaxy
Sagittarius

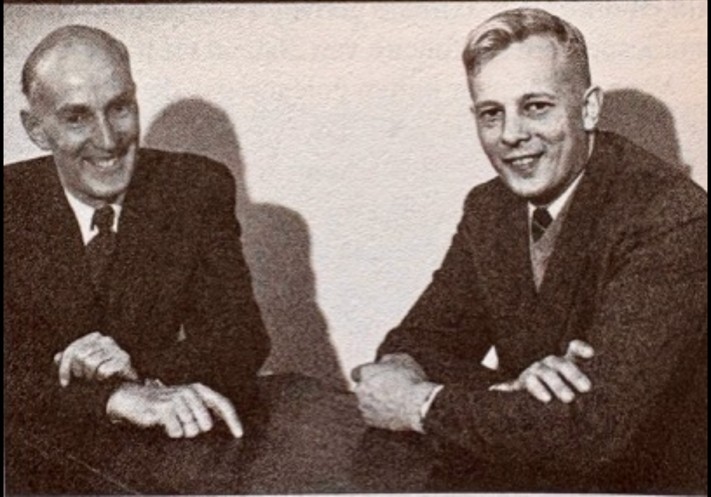

Ned. T. Natuurk. **11**, December 1945.

Radiogolven uit het wereldruim *)

door C. J. Bakker en H. C. van der Hulst

Zijn er ook afzonderlijke spectraallijnen?

21cm golven

de eis $S_m > 0{,}03$. Daar S_m meestal van de grootteorde 1 is, ziet de zaak er niet hopeloos uit, zelfs niet als we bedenken dat voor de gevoeligheid der huidige ontv... allaties de eis nog een factor 100 hoger moet gesteld word... ijn echter redenen om aan te nemen, dat de werkelijke S_m ... wat kleiner zal zijn. Zolang de strenge berekening nog niet gemaakt is, blijft het bestaan van deze lijn speculatief.

Hα-lijnen

Substitueren we de zo gevon... $\nu/\triangle\nu$, de juiste $h\nu/\varkappa T$ en $G_a/G = 0{,}78/8 = 0{,}1$ dan blijkt dat d... lijnen alle *onwaarneembaar* zijn.

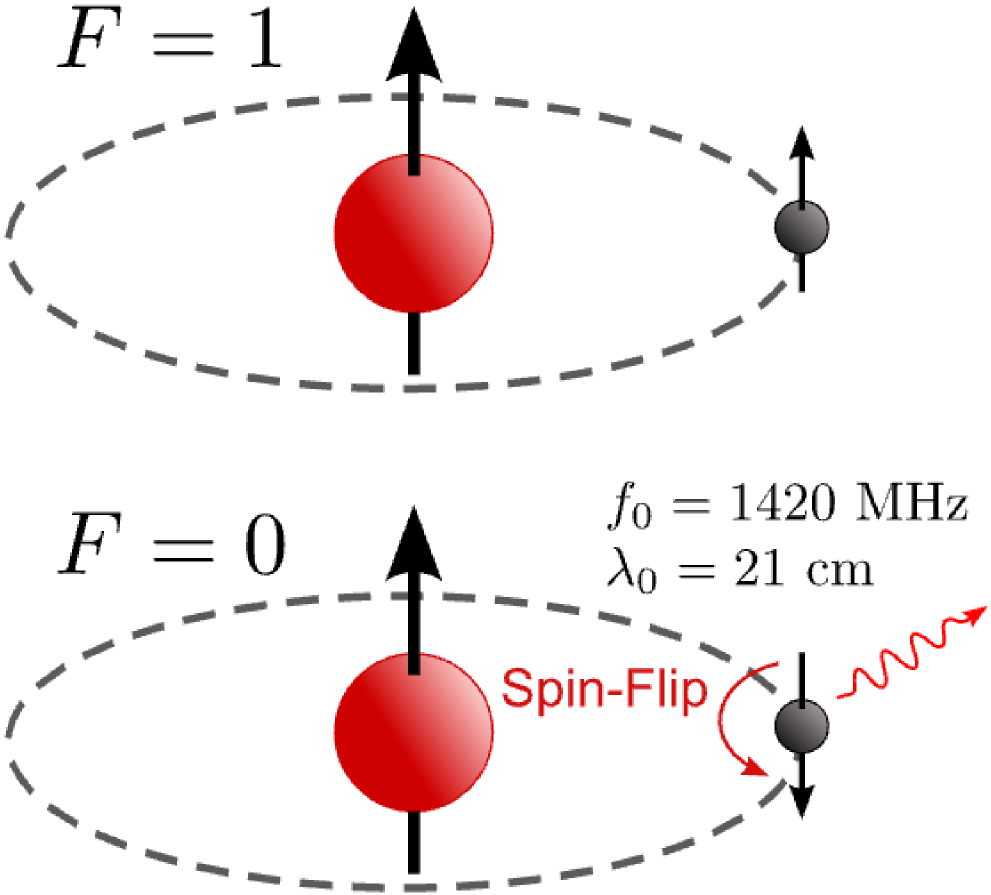
$F = 1$
$F = 0$
$f_0 = 1420$ MHz
$\lambda_0 = 21$ cm
Spin-Flip

356 NATURE September 1, 1951 Vol. 168

OBSERVATION OF A LINE IN THE GALACTIC RADIO SPECTRUM

Radiation from Galactic Hydrogen at 1,420 Mc./sec.

"Doc" Ewen
Ed Purcell

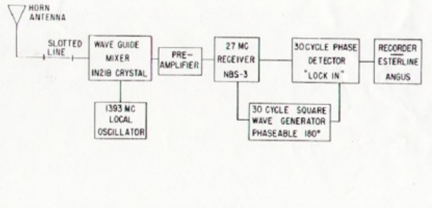

Figure 1. Block diagram of the equipment.

25 maart 1951
Lyman laboratory, Harvard

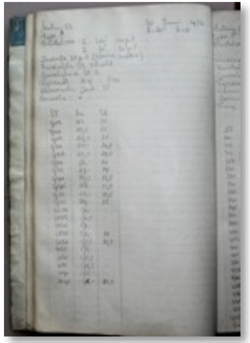

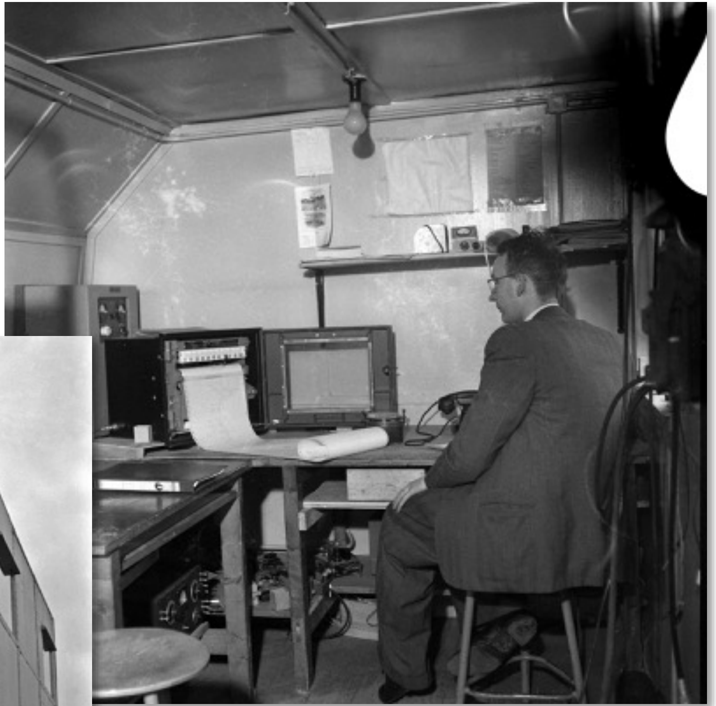

Lex Muller

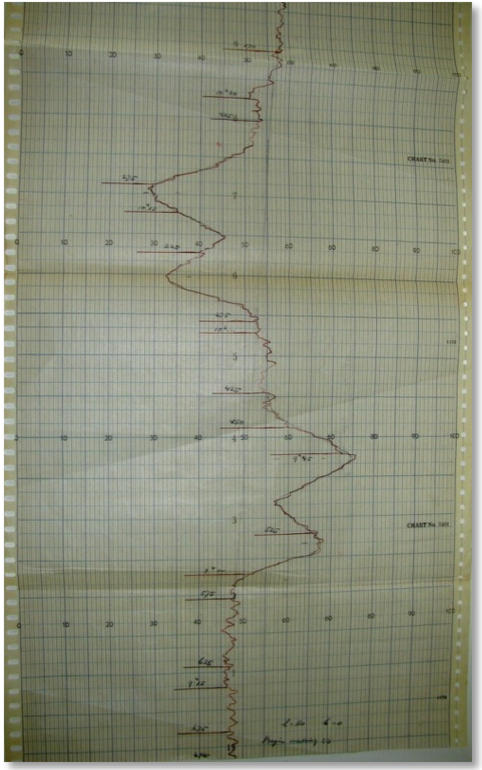

11 mei 1951
Kootwijk

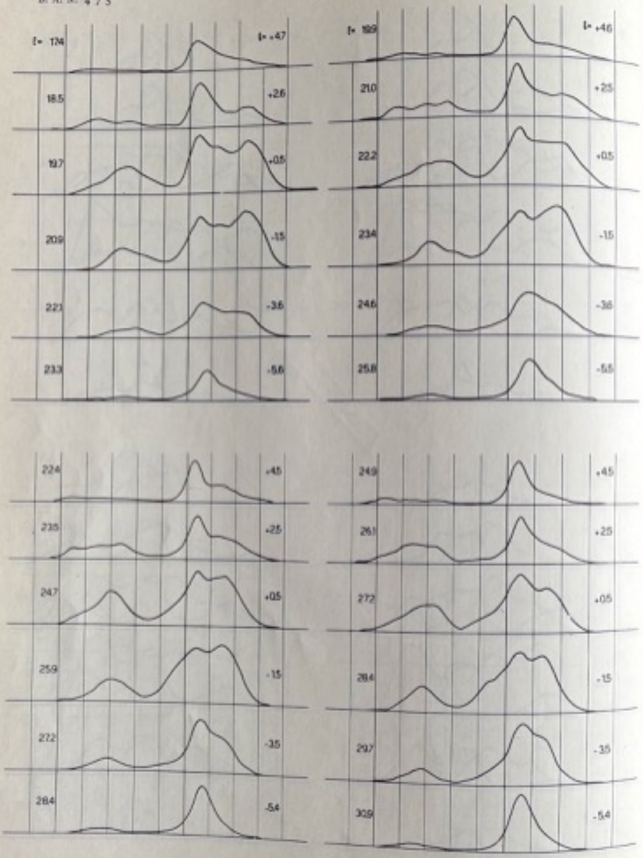
l = 17.4
18.5
19.7
20.9
22.1
23.3
b = +4.7
+2.6
+0.5
-1.5
-3.6
-5.6
l = 19.9
21.0
22.2
23.4
24.6
25.8
b = +4.6
+2.5
+0.5
-1.5
-3.6
-5.5
22.4
23.5
24.7
25.9
27.2
28.4
+4.5
+2.5
+0.5
-1.5
-3.5
-5.4
24.9
26.1
27.2
28.4
29.7
30.9
+4.5
+2.5
+0.5
-1.5
-3.5
-5.4

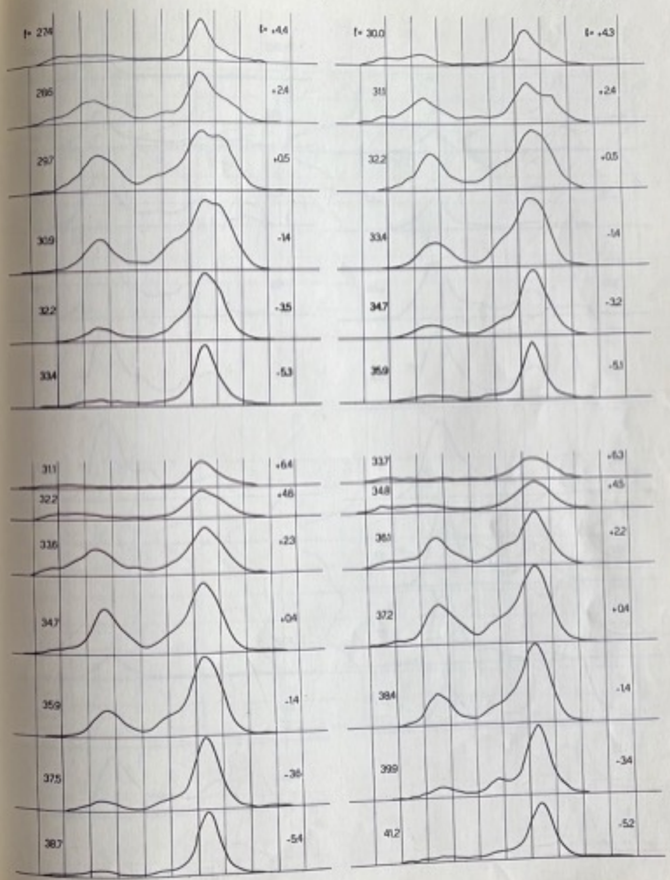
l = 27.4
28.6
29.7
30.9
32.2
33.4
b = +4.4
+2.4
+0.5
-1.4
-3.5
-5.3
l = 30.0
31.1
32.2
33.4
34.7
35.9
b = +4.3
+2.4
+0.5
-1.4
-3.2
-5.1
31.1
32.2
33.6
34.7
35.9
37.5
38.7
+6.4
+4.6
+2.3
+0.4
-1.4
-3.6
-5.4
33.7
34.8
36.1
37.2
38.4
39.9
41.2
+6.3
+4.5
+2.2
+0.4
-1.4
-3.4
-5.2

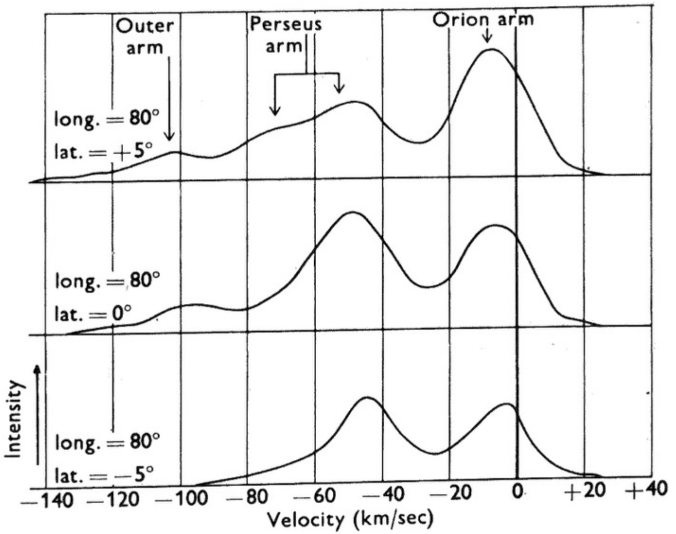

FIGURE 2 – *Line profiles for three points in Cassiopeia and Cepheus. Each profile is a plot of intensity against Doppler velocity. Their common longitude is 80° (broken line in figure 1). The middle point is in the galactic plane; the others have latitudes 5° above and below the galactic plane. Note different dependence on latitude in the three arms.*

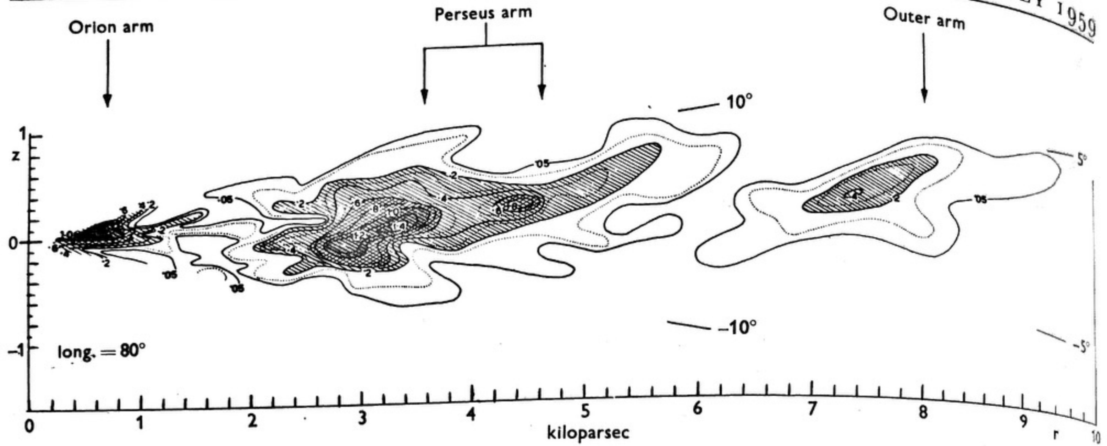

FIGURE 3 – *Cross-section perpendicular to the galactic plane. This shows isodensity contours of atomic hydrogen in a plane perpendicular to the galactic plane. The Sun (or Earth) is at the origin, r = distance from Sun along plane, z = distance from Sun perpendicular to plane. Heaviest shadings represent 2 atoms per cm³; the lowest contour represents 0·05 atom per cm³. Note here and in figure 2 that the Perseus arm is split and also that the outer arm lies above the galactic plane.*

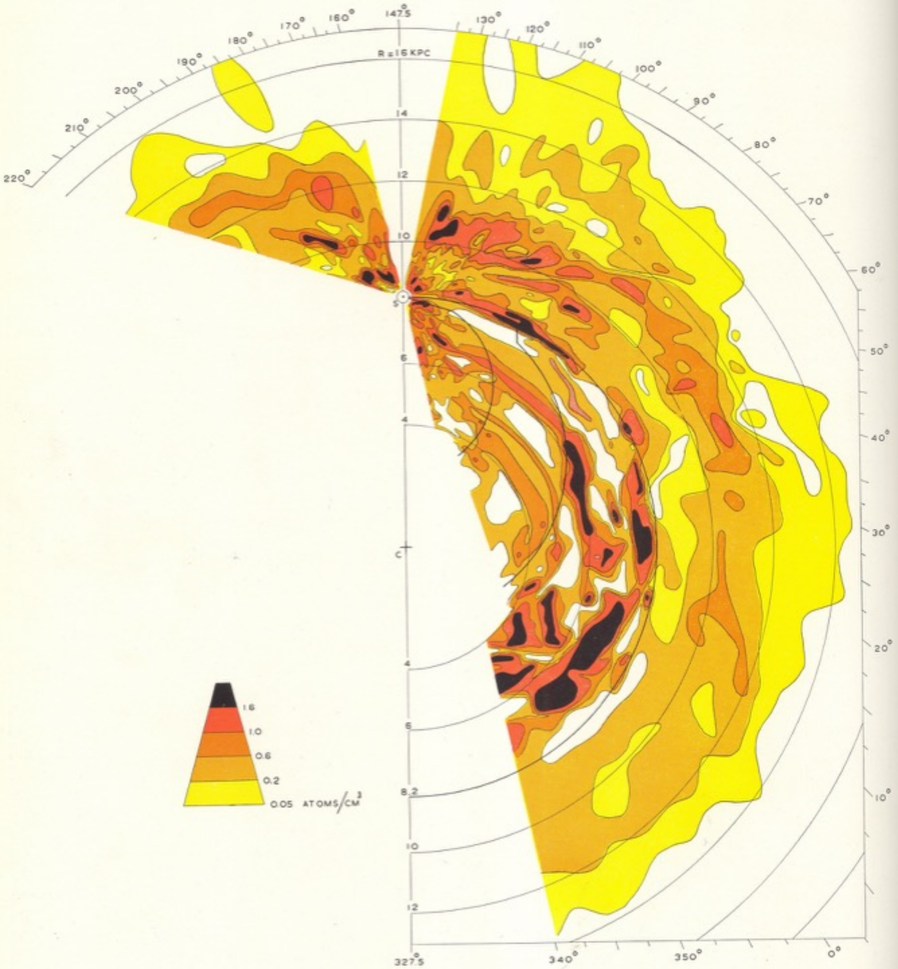

Contours of equal density of neutral hydrogen in the Galactic System. The maximum densities in the *z*-direction are projected on the galactic plane, and contours are drawn through the points.


1 july 1955


17 April 1956

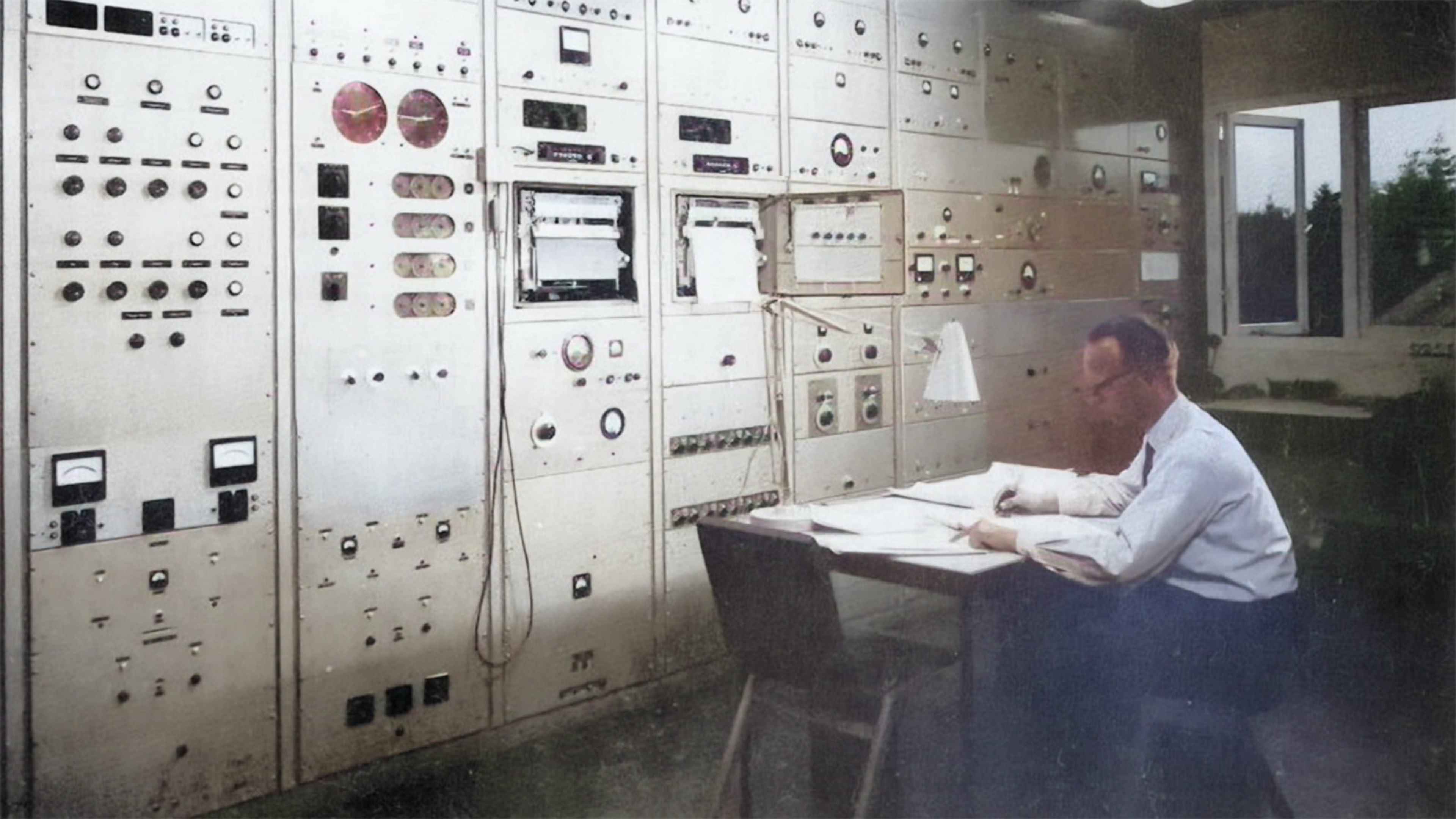

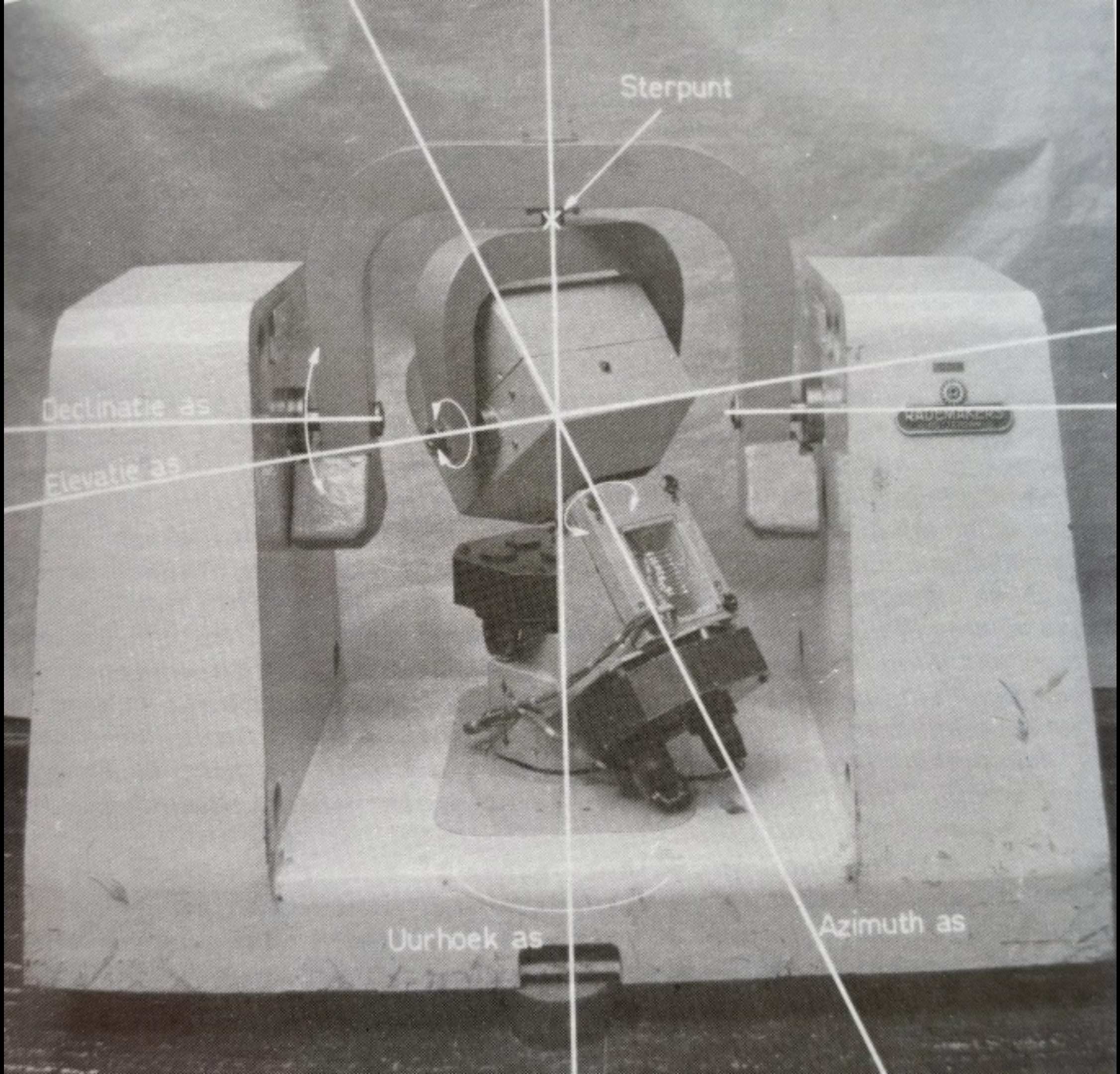
Sterpunt
Declinatie as
Elevatie as
Uurhoek as
Azimuth as

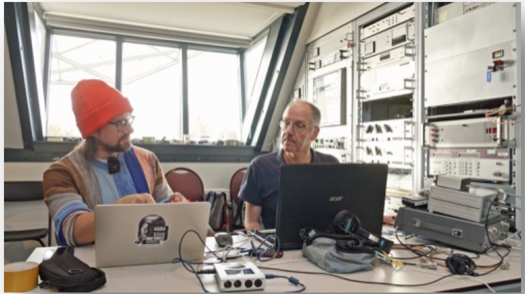

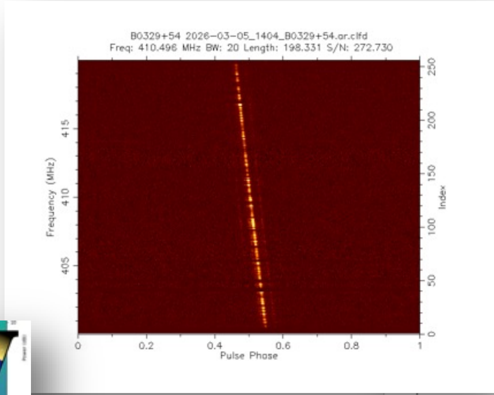
B0329+54 2026-03-05_1404_B0329+54.ar.clfd
Freq: 410.496 MHz BW: 20 Length: 198.331 S/N: 272.730
Frequency (MHz)
Index
Pulse Phase

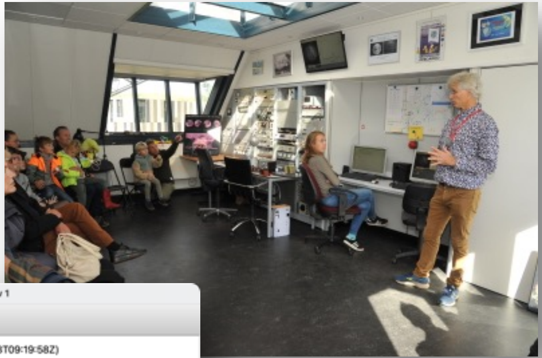

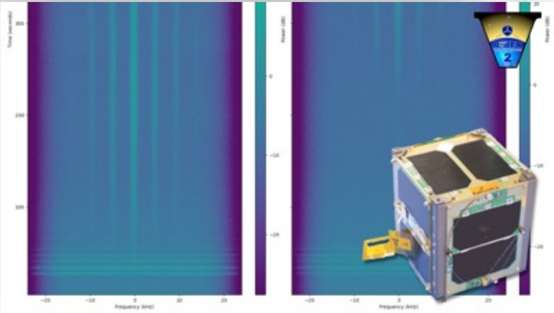

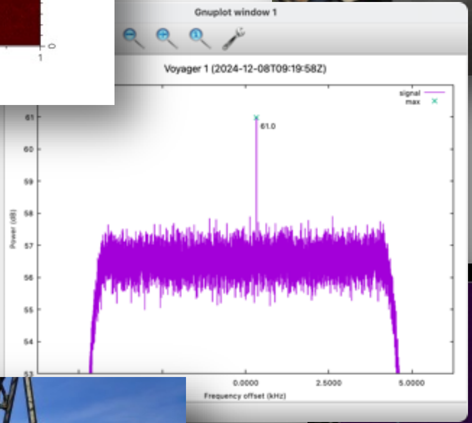
Gnuplot window 1
Voyager 1 (2024-12-08T09:19:58Z)
signal
max
61.0
Power (dB)
Frequency offset (kHz)

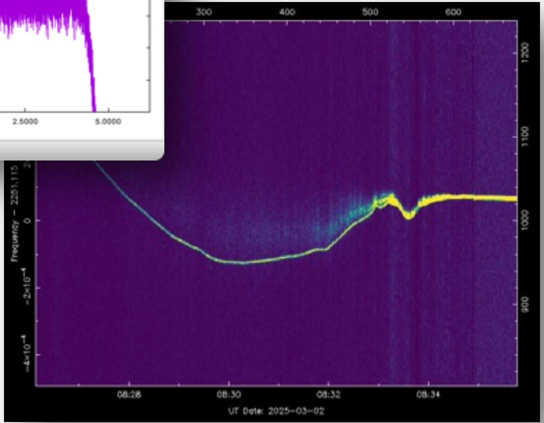
Frequency − 2261.115
UT Date: 2025-03-02

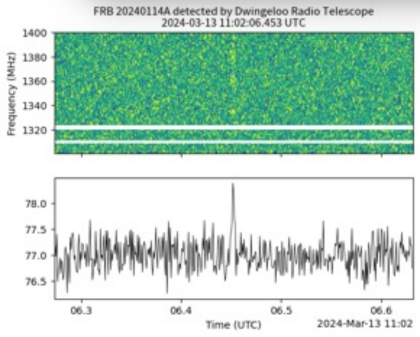
FRB 20240114A detected by Dwingeloo Radio Telescope
2024-03-13 11:02:06.453 UTC
Frequency (MHz)
Time (UTC)
2024-Mar-13 11:02

vrt-iq-tools

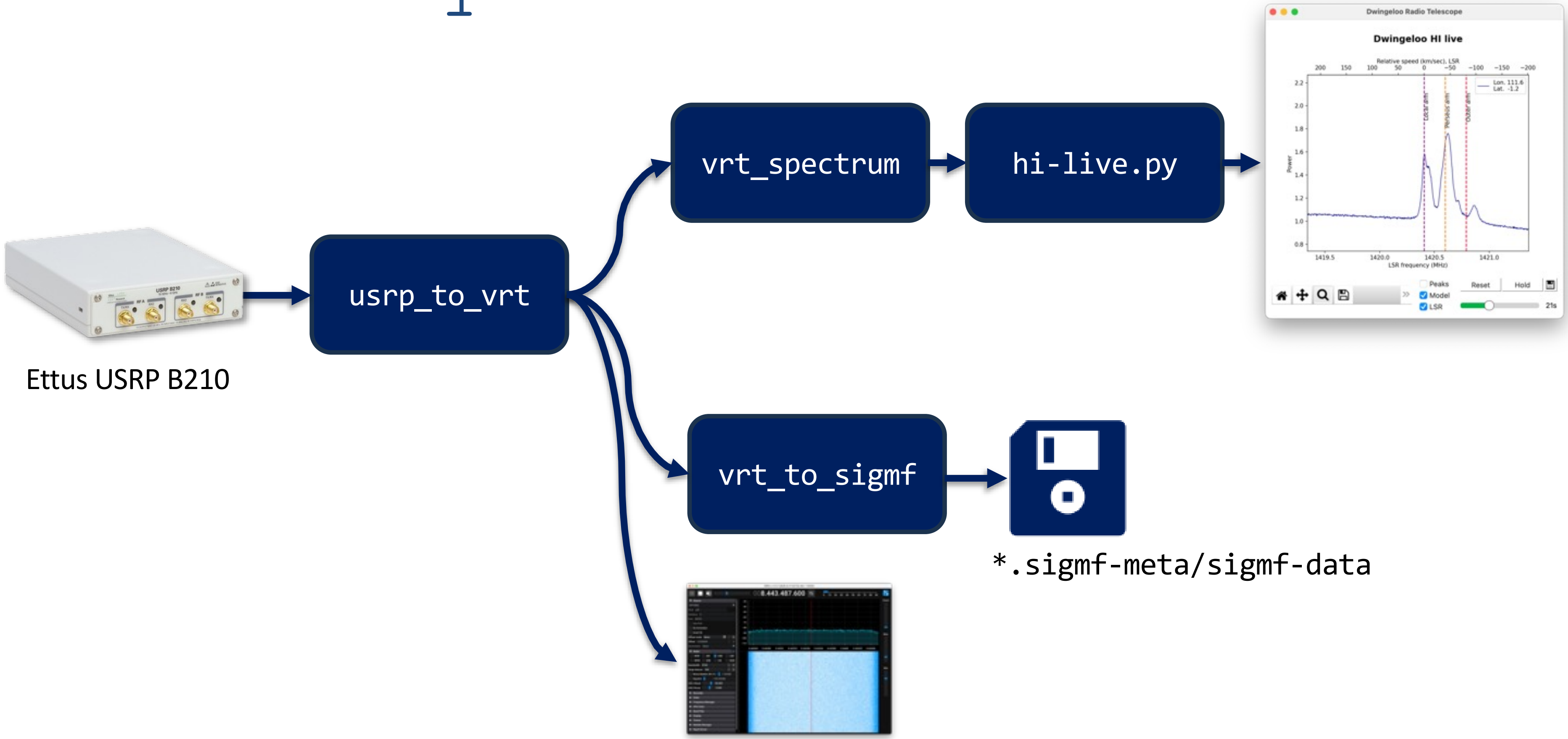

Ettus USRP B210
usrp_to_vrt
vrt_spectrum
hi-live.py
vrt_to_sigmf
*.sigmf-meta/sigmf-data
Dwingeloo Radio Telescope
Dwingeloo HI live

```
usrp_to_vrt --freq 1421.5e6 --rate 8e6 --gain 50 --ant RX2 --ref external --int-second --progress
```

vrt_spectrum

```
camrasdemo@mercurius:~$ ./vrt_spectrum --integration-time 1 --int-second --num-bins 5 --dt-trace
# VRT Context:
#     Stream ID (channel): 1 (0)
#     Sample Rate [samples per second]: 8000000
#     RF Freq [Hz]: 1421500000
#     Bandwidth [Hz]: 56000000
#     Gain [dB]: 70
#     Ref lock: external
#     Time cal: internal
# Spectrum parameters:
#     Bins: 5
#     Bin size [Hz]: 1600000.00
#     Integrations: 1600000
#     Integration Time [sec]: 1.00
timestamp, azimuth, elevation, 1418300000, 1419900000, 1421500000, 1423100000, 1424700000
1681495831.000006031, 153.506, 28.589, 54.911, 55.740, 55.908, 55.924, 55.789
1681495832.000006031, 153.508, 28.587, 54.916, 55.743, 55.917, 55.922, 55.787
1681495833.000006031, 153.510, 28.586, 54.912, 55.739, 55.906, 55.926, 55.792
1681495834.000006031, 153.512, 28.585, 54.920, 55.741, 55.905, 55.925, 55.786
1681495835.000006031, 153.514, 28.584, 54.908, 55.738, 55.914, 55.925, 55.792
1681495836.000006031, 153.516, 28.583, 54.914, 55.740, 55.915, 55.927, 55.791
```

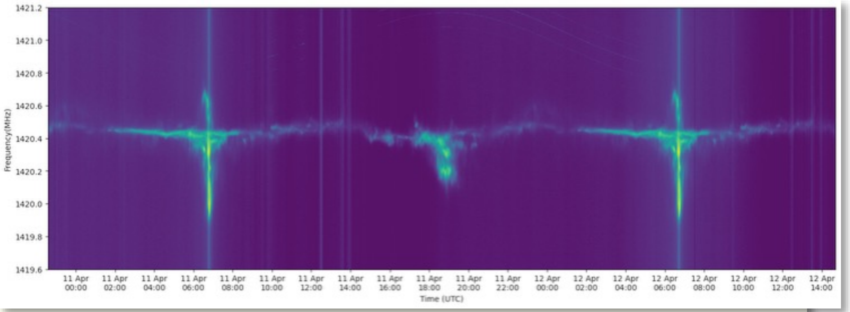

[2]:
```
data = Table.read('/home/telkamp/data/2026-01-17/woerden-cloud.ecsv', format='ascii.ecsv')
```

[3]:
```
start_col = int(data.meta['spectrum']['col_first_bin'])
freqs = np.array(list(map(int,data.columns[start_col:])))
fc = data.meta['vrt']['frequency']
```

[4]:
```
spec_data = np.column_stack([data[colname] for colname in data.columns[start_col:]])
print(spec_data.shape)
```

```
(60, 6000)
```

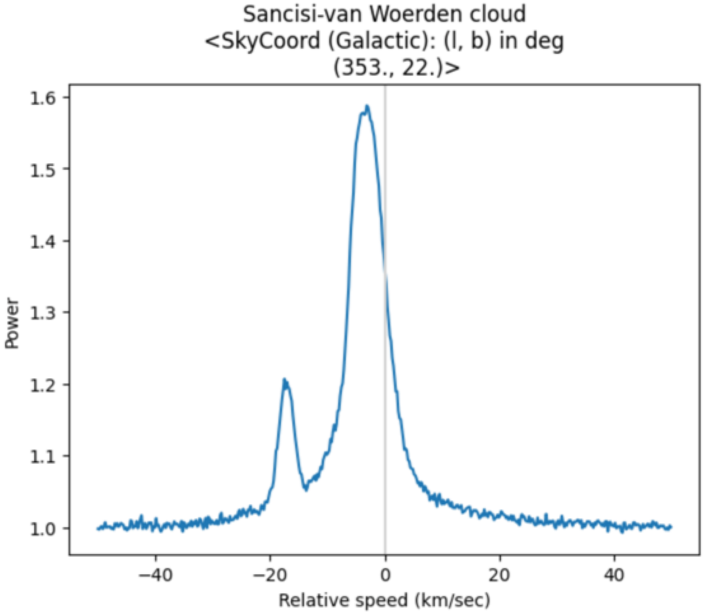

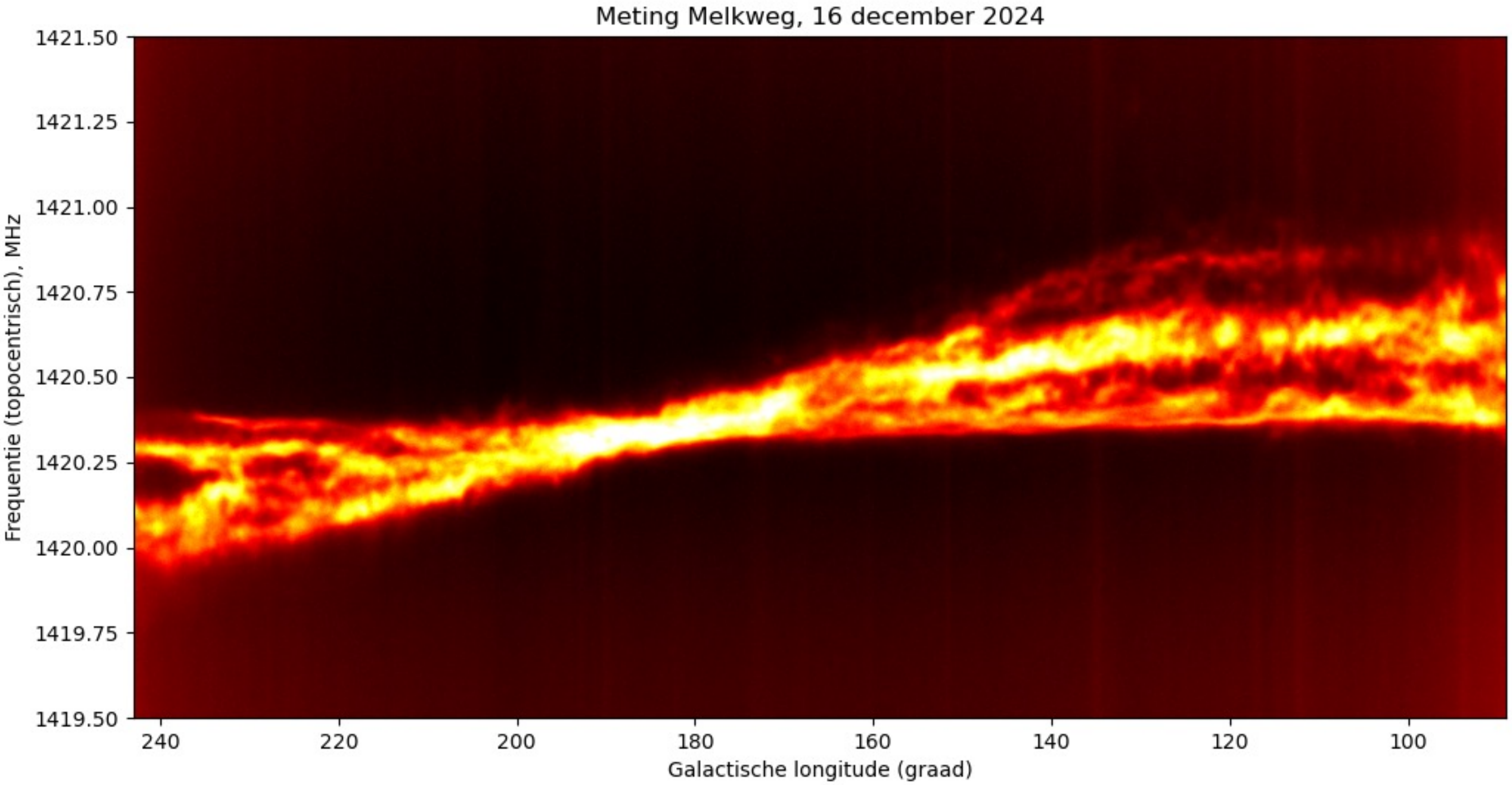
Meting Melkweg, 16 december 2024
1421.50
1421.25
1421.00
1420.75
1420.50
1420.25
1420.00
1419.75
1419.50
Frequentie (topocentrisch), MHz
240
220
200
180
160
140
120
100
Galactische longitude (graad)

NETHERLANDS FOUNDATION FOR RADIO ASTRONOMY
RADIO OBSERVATORY, DWINGELOO
KAPTEYN ASTRONOMICAL LABORATORY, GRONINGEN
OBSERVATORY, LEIDEN

SUMMARY OF OBSERVATIONS OF THE 21-cm LINE OF NEUTRAL HYDROGEN MADE WITH THE 25-m RADIO TELESCOPE AT DWINGELOO, THE NETHERLANDS before the 31st of October, 1961.

by

E. Raimond.

TABLE I

object	program number	investigator	type of meas.	coord. system	limits in l or α: lower	limits in l or α: upper	limits in b or δ: lower	limits in b or δ: upper	spacing: in l or α	spacing: in b or δ	approx. limits of frequency-interval with respect to LSR: lower	approx. limits of frequency-interval with respect to LSR: upper	spacing in freq.	$B_{1/2}$	number of meas. per profile or sweep: independent	number of meas. per profile or sweep: total	number of profiles or sweeps	receiver	dates	computer-readable: data	computer-readable: form
1	2	3	4	5	6	6	7	7	8	8	9	9	10	11	12	12	13	14	15	16	16
					°	°	°	°	°	°	km/s	km/s	kc/s	kc/s							
Central region of galaxy	15	DDD	A	1	320.0	325.5	-2.0	-0.5	0.5	0.5	-1500	+1500	20	16	1-2	1-2	44	8	jan-feb 59		
			A	1	320.0	330.0	-3.0	-2.5	0.5	0.5	0	+ 500	10	16	1	2	43	8	mrch-jun 61	T_b	cards
			A	1	320.0	330.0	0.0	+0.5	0.5	0.5	0	+ 500	10	16	1	2	42	8	mrch-jun 61	T_b	cards
			C	1	326.0	330.0	-2.0	-0.5	0.25	0.25	+1000	+1200	≤50	16	1-2	1-2	119	8	mrch-oct 59		
			A	1	330.5	333.5	-2.0	-0.5	0.5	0.5	-1500	+ 500	20	39	1-2	1-2	28	1	jan-feb 59		
			A	1	334.0	337.0	-0.5	-0.5	0.5	0.25	-1500	- 150	20	16	1-2	1-2	63	8	jul-aug 58		
			A	1	331.5	350.0	-2.0	-1.0	0.5	0.5	-1500	- 150	20	39	1-2	1-2	78	1	nov-dec 57		
NGC 6611	13	DHS	A	1	342.51	343.51	-2.64	-1.74	0.5	0.5	- 300	+ 100	5	8	1-2	2-3	7	8	mrch-apr 59		
M 8(NGC 6523)			A	1	333.22	334.22	-3.13	-2.23	0.5	0.5	- 300	+ 200	5	8	1-2	2-3	7	8	mrch-apr 59		
NGC 6357			A	1	320.20	321.30	-0.65	-0.65	0.25	0	- 300	+ 200	5	8	1-2	2-3	7	8	mrch-apr 59		
Expansion test	11	LB	B_p	2	-5.0	+1.0	-5.0	+5.0	1.0	0.25	- 200	+ 200	25	16	2	2	80	8	jun-sep 61	T_b	cards
			B_p	2	+1.0	+5.0	-5.0	+5.0	1.0	0.25	- 200	+ 200	25	16	2	2	80	8	jun-sep 61	T_b	cards
Scorpius (II Sco)	19	BvW	A	1	318.0	326.0	+15.0	+19.0	≤ 1.0	≤ 1.0	- 250	+ 200	10	10	1	1	55	1	oct 56-sep57		
			A	1	318.0	326.0	+15.0	+19.0	≤ 0.7	≤ 0.7	- 450	+ 400	5	8	2	2	110	8	jan59-apr60	T	tape
											- 250, or 200										
Ophiuchus-Aquila (Region 3C...)	01	ABB DD	A	1	330.0	10.0	-21.5	-27.5	2.0	0	- 600	+ 200	10	16	1	2	11	8	may-sep 61	T_b	cards
			A	1	5.0	10.0	-19.5	-14.5	≤1.0	≤1.0	- 600	+ 200	10	16	1	2	56	8	may-sep 61	T_b	cards
			A	1	351.0	10.0	-16.5	-16.5	1.0	0	- 600	+ 200	10	16	1	2	21	8	may-sep 61	T_b	cards
			A	1	350.0	10.0	-13.5	-11.5	1.0	1.0	- 600	+ 200	10	16	1	2	65	8	may-sep 61	T_b	cards
			A	1	350.0	10.0	-10.5	- 7.5	1.0	1.0	- 800	0	10	16	1	2	92	8	sep58-jul59 and may-sep 61	T_b	cards
			A	1	350.0	10.0	- 6.5	+ 3.5	1.0	0.5	- 800	0	10	16	1	2	447	8	sep58-aug59	T_b	cards
			A	1	350.0	10.0	+ 1.5	+ 1.5	1.0	0	- 800	0	2.5	8	1	2	21	8	sep58-aug59	T_b	cards
			A	1	350.0	10.0	+ 4.5	+ 7.5	1.0	1.0	- 800	0	10	16	1	2	82	8	sep58-aug59 and may-sep 61	T_b	cards
			A	1	350.0	10.0	+ 8.5	+10.5	1.0	1.0	- 600	+ 200	10	16	1	2	63	8	may-sep 61	T_b	cards
			A	1	350.0	10.0	+12.0	+12.0	2.0	0	- 600	+ 200	10	16	1	2	11	8	may-sep 61	T_b	cards
			A	1	350.0	10.0	+13.5	+13.5	1.0	0	- 600	+ 200	10	16	1	2	21	8	may-sep 61	T_b	cards
			A	1	350.0	10.0	+18.5	+18.5	2.0	0	- 600	+ 200	10	16	1	2	11	8	may-sep 61	T_b	cards
			B_p	1	350.0	10.0	≤- 9.5	≥+ 6.5	1.0	0.25	- 800	0	25	16	1	1	500	8	sep58-mrch59	T_b	cards
Determination of rotation curve	12	GW	A	2	42.0	70.0	0	0	1.0	0	- 800	0	5	8	1	2	19	8	nov-dec 61	T_b	cards
Outer spiral arm	06	KTH	A	1	10.0	10.0	-15.0	+ 5.0	0	1.0	+ 100	+ 500	10	16	1	2	27	8	jul-sep 61	T_b	cards
			B_p	1	10.0	10.0	+ 5.0	+25.0	0	0.25	+ 100	+ 500	25	16	1	1	16	8	apr-jun 61	T_b	cards
			A	1	15.0	15.0	+ 5.0	+25.0	0	1.0	+ 100	+ 500	10	16	1	2	27	8	jul-sep 61	T_b	cards
			B_p	1	20.0	20.0	+ 5.0	+25.0	0	0.25	+ 150	+ 550	25	16	1	1	16	8	apr-jun 61	T_b	cards
			A	1	25.0	25.0	+ 5.0	+25.0	0	1.0	+ 200	+ 600	10	16	1	2	27	8	jul-sep 61	T_b	cards
			A	1	30.0	30.0	+ 5.0	+17.0	0	1.0	+ 250	+ 650	10	16	1	2	9	8	jul-sep 61	T_b	cards
			B_p	1	30.0	30.0	+25.0	+25.0	0	0.25	+ 250	+ 650	25	16	1	1	16	8	apr-jun 61	T_b	cards
			A	1	35.0	35.0	+ 5.0	+ 9.0	0	1.0	+ 250	+ 650	10	16	1	2	9	8	jul-sep 61	T_b	cards
			B_p	1	35.0	35.0	+10.0	+25.0	0	0.25	+ 250	+ 650	25	16	1	1	16	8	apr-jun 61	T_b	cards
			A	1	40.0	40.0	+ 5.0	+25.0	0	1.0	+ 250	+ 650	10	16	1	2	11	8	jul-sep 61	T_b	cards
			A	1	40.0	40.0	+26.0	+30.0	0	1.0	+ 250	+ 650	10	16	1	2	3	8	jul-sep 61	T_b	cards
			A	1	45.0	45.0	+ 5.0	+ 8.0	0	1.0	+ 300	+ 700	10	16	1	2	13	8	jul-sep 61	T_b	cards
			B_p	1	45.0	45.0	+10.0	+30.0	0	0.25	+ 300	+ 700	25	16	1	1	16	8	apr-jun 61	T_b	cards
			B_p	1	50.0	50.0	+ 5.0	+30.0	0	0.25	+ 300	+ 700	25	16	1	1	16	8	apr-jun 61	T_b	cards
			A	1	50.0	50.0	+ 5.0	+25.0	0	1.0	+ 300	+ 700	10	16	1	2	11	8	jul-sep 61	T_b	cards
			B_p	1	55.0	55.0	+15.0	+35.0	0	0.25	+ 300	+ 700	25	16	1	1	16	8	apr-jun 61	T_b	cards
			B_p	1	60.0	60.0	+ 5.0	+25.0	0	0.25	+ 350	+ 750	25	16	1	1	16	8	apr-jun 61	T_b	cards
			A	1	60.0	60.0	+26.0	+50.0	0	1.0	+ 350	+ 750	10	16	1	2	16	8	jul-sep 61	T_b	cards
			A	1	65.0	65.0	+ 5.0	+35.0	0	1.0	+ 350	+ 750	10	16	1	2	31	8	jul-sep 61	T_b	cards
			B_p	1	70.0	70.0	+ 5.0	+25.0	0	0.25	+ 350	+ 750	25	16	1	1	16	8	apr-jun 61	T_b	cards
			A	1	70.0	70.0	+26.0	+40.0	0	1.0	+ 350	+ 750	10	16	1	2	13	8	jul-sep 61	T_b	cards
			A	1	75.0	75.0	+ 5.0	+40.0	0	1.0	+ 350	+ 750	10	16	1	2	36	8	jul-sep 61	T_b	cards
			B_p	1	80.0	80.0	+25.0	+25.0	0	0.25	+ 350	+ 750	25	16	1	1	16	8	apr-jun 61	T_b	cards
			A	1	80.0	80.0	+26.0	+40.0	0	1.0	+ 350	+ 750	10	16	1	2	13	8	jul-sep 61	T_b	cards
			A	1	85.0	85.0	+ 5.0	+40.0	0	1.0	+ 300	+ 700	10	16	1	2	36	8	jul-sep 61	T_b	cards
			B_p	1	90.0	90.0	+ 5.0	+25.0	0	0.25	+ 300	+ 700	25	16	1	1	16	8	apr-jun 61	T_b	cards
			A	1	90.0	90.0	+26.0	+40.0	0	1.0	+ 300	+ 700	10	16	1	2	13	8	jul-sep 61	T_b	cards
			A	1	95.0	95.0	+ 5.0	+ 8.0	0	1.0	+ 300	+ 700	10	16	1	2	4	8	jul-sep 61	T_b	cards
			B_p	1	95.0	95.0	+10.0	+40.0	0	0.25	+ 300	+ 700	25	16	1	1	16	8	apr-jun 61	T_b	cards
			B_p	1	100.0	100.0	+ 5.0	+25.0	0	0.25	+ 300	+ 700	25	16	1	1	16	8	apr-jun 61	T_b	cards
			A	1	100.0	100.0	+26.0	+40.0	0	1.0	+ 300	+ 700	10	16	1	2	13	8	jul-sep 61	T_b	cards
			A	1	105.0	105.0	+ 5.0	+ 5.0	0	1.0	+ 300	+ 700	10	16	1	2	1	8	jul-sep 61	T_b	cards
			B_p	1	105.0	105.0	+10.0	+40.0	0	0.25	+ 250	+ 650	25	16	1	1	16	8	apr-jun 61	T_b	cards
			A	1	110.0	110.0	+15.0	+ 4.0	0	1.0	+ 200	+ 600	10	16	1	2	25	8	jul-sep 61	T_b	cards
			B_p	1	110.0	110.0	+ 5.0	+25.0	0	0.25	+ 200	+ 600	25	16	1	1	16	8	apr-jun 61	T_b	cards
			A	1	110.0	110.0	+26.0	+40.0	0	1.0	+ 200	+ 600	10	16	1	2	15	8	jul-sep 61	T_b	cards
Surroundings l=50, b=0	20	BvW SS	A	8	309.35	310.5	+40.35	+43.05	0.25	0.25	- 100	+ 300	5	8	2	1	7	8	jul 59		
			B_p	8	306.2	313.2	+40.3	+43.3	0.25	0.5	- 24	+ 10	-	38	2	2	11	1	jul-aug57 & jul59		
			B_p	8	306.2	313.2	+40.3	+43.3	0.50	0.55	- 24	+ 10	-	38	2	2	15	1	jul-aug57 & jul59		

TABLE I (continued)

object	program number	investigator	type of meas.	coord. system	limits in l or α: lower	limits in l or α: upper	limits in b or δ: lower	limits in b or δ: upper	spacing: in l or α	spacing: in b or δ	approx. limits of frequency-interval with respect to LSR: lower	approx. limits of frequency-interval with respect to LSR: upper	spacing in freq.	$B_{1/2}$	number of meas. per profile or sweep: independent	number of meas. per profile or sweep: total	number of profiles or sweeps	receiver	dates	computer-readable: data	computer-readable: form
1	2	3	4	5	6	6	7	7	8	8	9	9	10	11	12	12	13	14	15	16	16
					°	°	°	°	°	°	km/s	km/s	kc/s	kc/s							
Perseus Cassiopeia Andromeda	17	BvW	A	1	54.0	138.0	-15.0	-6.0	≤ 1.0	≤ 1.0	- 200	+ 650	5	8	2	2	100	8	nov58-apr59		
Perseus Cassiopeia	07	BvW	A	1	100.0	105.0	- 5.0	+2.0	≤ 1.0	≤ 1.0	- 200	+ 650	5	8	1	1-3	37	8	jun-aug 58		
			A	2	131.0	137.0	- 6.0	0.0	≥ 0.7	≥ 0.7	- 200	+ 650	5	8	1	2		8	mrch-sep 61	T_b	cards
Surroundings $l_{II}=131°$, $b_{II}=-1°$	16	BvW	A	2	130.75	131.25	- 1.25	-0.75	≥ 0.1	≥ 0.1	- 100	+ 350	5	8	1-2	2-4	15	8	apr 61	T_b	cards
Anticenter of galaxy	08	PGL	A	2	173.0	185.0	-10.0	-8.0	1.0	1.0	- 300	+ 250	5	8	1	2	39	8	apr-aug 61	T_b	cards
			A	2	186.0	191.0	-11.0	+5.0	1.0	1.0	- 400	+ 350	5	8	1	2	10	8	apr-aug 61	T_b	cards
			A	2	174.0	183.0	-15.0	+8.0	5.0	1.0	≥ - 400	≤ + 350	5	8	1	2	89	8	apr-aug 61	T_b	cards
			A	2	219.0	221.0	-12.0	-8.0	5.0	1.0	≥ - 450	≤ + 150	5	8	1	2	25	8	apr-aug 61	T_b	cards
			A	2	225.0	231.0	-16.0	-13.0	4.0	1.0	≥ - 450	≤ + 150	5	8	1	2	6	8	apr-aug 61	T_b	cards
			A	2	225.0	225.0	- 7.0	+5.0	0	1.0	≥ - 450	≤ + 150	5	8	1	2	5	8	apr-aug 61	T_b	cards
Supernova (I+II Sco)	02	DD	B_p	2	54.0	105.0	+4.0	+13.0	0.25	≤ 1.0	- 250	+ 150	18	8	1	1	300	8	jul-aug 58	T_b	cards
			B_p	2	56.5	101.25	+4.0	+13.0	≥ 0.75	0.25	- 250	+ 150	18	8	1	1	160	8	jul-aug 58	T_b	cards
			A	1	160.0	180.0	-8.0	+10.0	1.0	1.0	≥ - 450	≤ + 250	5	8	1-2	2-3	399	8	jan-jul 59 apr-sep 61	T_b	cards
			A	1	168.0	172.0	+6.5	+ 4.5	0.5	0.5	≥ - 450	≤ + 250	5	8	2	3	61	8	jun-jul 59	T_b	cards
			A	1	172.5	175.5	+2.0	+ 1.0	0.5	0.5	≥ - 450	≤ + 250	5	8	2	3	37	8	jun-jul 59	T_b	cards
			A	1	160.0	186.0	-10.0	+ 9.0	3.0	1.0	≥ - 450	≤ + 250	5	8	1	2	27	8	apr-sep 61	T_b	cards
Orion	04	BvW	A	1	171.0	178.0	-20.0	-14.0	0.5	0.5	- 250	+ 200	10	19	2	2	200	1	oct58-apr58		
			A	1	170.0	180.0	-13.0	- 9.0	1.0	1.0	- 450	+ 400	5	8	1-2	2-4	55	8	nov58 and apr60	T	tape
			A	1	170.0	180.0	-23.0	-16.0	≤ 0.7	≤ 0.7	- 450	+ 400	5	8	1-2	2-4	201	8	nov59 and apr60	T	tape
			A	1	170.0	180.0	-23.0	-14.0	≥ 1.0	≥ 1.0	- 250	+ 200	2.5	4	1	1-2	14	8	apr 60		
Orion surroundings	19	BvW	A	1	172.5	172.5	-25.0	- 9.0	0	≥ 0.5	- 250	+ 200	10	19	1	1	72	1	aug-sep 5?		
			A	1	175.0	175.0	-25.0	- 9.0	0	≥ 0.5	- 250	+ 200	10	19	1	1					
			A	1	170.0	180.0	-17.5	-17.5	0.5	0	- 250	+ 200	10	19	1	1					
			B_p	1	150.0	175.0	-25.0	-20.0	0.5	1.0	- 250	+ 200	10	16	1	1	200	8	jul 59-feb 60		
			B_p	1	150.0	200.0	-19.0	- 9.0	0.5	1.0	- 250	+ 200	10	16	1	1	400	8	jul 59-feb 60		
			B_p	1	168.0	180.0	-20.0	+30.0	1.0	0.5	- 250	+ 200	10	16	1	1	600	8	jul 59-feb 60		
Intermediate latitudes survey	05	BvW KT LB	A	1	340.0	200.0	-20.0	-20.0	10.0	0	length	800	5	8	2	2	25	8	jul 58-apr60	T	tape
			A	1	340.0	200.0	-15.0	-15.0	10.0	0	length	800	5	8	2	2	25	8	jul 58-apr60	T	tape
			A	1	343.0	195.0	-10.0	-10.0	15.0	0	length	800	5	8	2	2	15	8	jul 58-apr60	T	tape
			A	1	350.0	170.0	-10.0	-10.0	30.0	0	length	800	5	8	2	2	7	8	jul 58-apr60	T	tape
			A	1	328.0	208.0	+10.0	+10.0	15.0	0	length	800-1200	5	8	2	2	17	8	jul 58-apr60	T	tape
			A	1	320.0	200.0	+10.0	+10.0	30.0	0	length	800-1200	5	8	2	2	9	8	jul 58-apr60	T	tape
			A	1	20.0	170.0	+10.0	+10.0	10.0	0	length	800-1200	5	8	2	2	10	8	jul 58-apr60	T	tape
			A	1	320.0	200.0	+15.0	+15.0	10.0	0	length	800	5	8	2	2	27	8	jul 58-apr60	T	tape
			A	1	320.0	230.0	+20.0	+20.0	10.0	0	length	800	5	8	2	2	28	8	jul 58-apr60	T	tape
			A	1	310.0	230.0	+25.0	+25.0	10.0	0	length	800	5	8	2	2	28	8	jul 58-apr60	T	tape
			A	1	65.0	165.0	+25.0	+25.0	5.0	0	length	800	5	8	1	2	15	8	mrch 61	T_b T	cards and tape
Intermediate latitudes & refinement	14	BvW KT	A	1	0.0	20.0	-15.0	+15.0	2.0	0	- 800	+ 800	5	8	3	3	11	8	dec 59	T	tape
			A	1	10.0	10.0	-40.0	+40.0	0	1.0	- 800	+ 800	5	8	3	3	10	8	dec 59	T	tape
B			A	1	60.0	80.0	+15.0	+15.0	≤ 2.0	0	length	800	5	8	2	2	28	8	nov-dec 59	T	tape
			A	1	70.0	70.0	+10.0	+20.0	0	≤ 1.0	length	800	5	8	2	2	15	8	nov-dec 59	T	tape
C			A	1	90.0	110.0	+15.0	+15.0	2.0	0	length	800	5	8	2	2	11	8	nov 59	T	tape
			A	1	100.0	100.0	+10.0	+20.0	0	1.0	length	800	5	8	2	2	10	8	nov 59	T	tape
D			A	1	90.0	110.0	+25.0	+25.0	1.0	0	length	800	5	8	2	2	21	8	mrch 61	T_b	cards and
			A	1	100.0	100.0	+20.0	+30.0	0	1.0	length	800	5	8	2	2	10	8	mrch 61	T	tape
High latitudes	03	SB	C	1	327.0	327.0	+60.0	+90.0	90.0	10.0	- 900	+ 900	50	20	4-6	4-6	13	8	dec 59		
			C	1	327.0	327.0	+60.0	+90.0	90.0	10.0	- 900	+ 900	400	160	4-6	4-6	13	1	dec 59		
			A	1	0.0	190.0	-40.0	-40.0	10.0	0	- 800	+ 800	5	8	2	2	20	8	aug-sep 61	T_b	cards
			A	1	0.0	360.0	+40.0	+40.0	10.0	0	- 800	+ 800	5	8	2	2	36	8	aug-sep 61	T_b	cards
Absorption profiles Cas A	09	GAH	A	E	350.39	350.39	+58.57	+58.57	0	0	- 145	+ 600	2.5 / 5	5 / 8	2 / 2	2 / 2	2	1	feb-apr 58		
			A	E	348.09	350.00	+58.60	+58.68	4.0	0	- 145	+ 600	5	8	2	2	2	1	feb-apr 58		
			B_p	E	346.0	356.0	+58.60	+58.68	0.25	0	- 84	+ 305	10	8	1	1	42	1	feb-apr 58		
Cyg A			A	E	299.51	299.51	+40.61	+40.61	0	0	- 310	+ 700	2.5 / 5	5 / 8	2 / 2	2 / 2	2	1	feb-apr 58		
			A	E	298.70	300.38	+39.88	+41.42	1.60	1.60	- 310	+ 700	5	8	2	2	2	1	feb-apr 58		
			B_p	E	297.0	302.4	+40.61	+40.61	0.25	0	- 300	+ 750	10	8	1	1	106	1	feb-apr 58		
Tau A			A	E	83.00	83.00	+21.99	+21.99	0	0	- 200	+ 200	2.5 / 5	5 / 8	2 / 2	2 / 2	2	1	feb-apr 58		
			A	E	82.00	84.00	+22.08	+22.08	2.0	0	- 200	+ 200	5	8	2	2	2	1	feb-apr 58		
			B_p	E	79.5	86.5	+21.99	+21.99	0.25	0	- 200	+ 200	10	8	1	1	41	1	feb-apr 58		

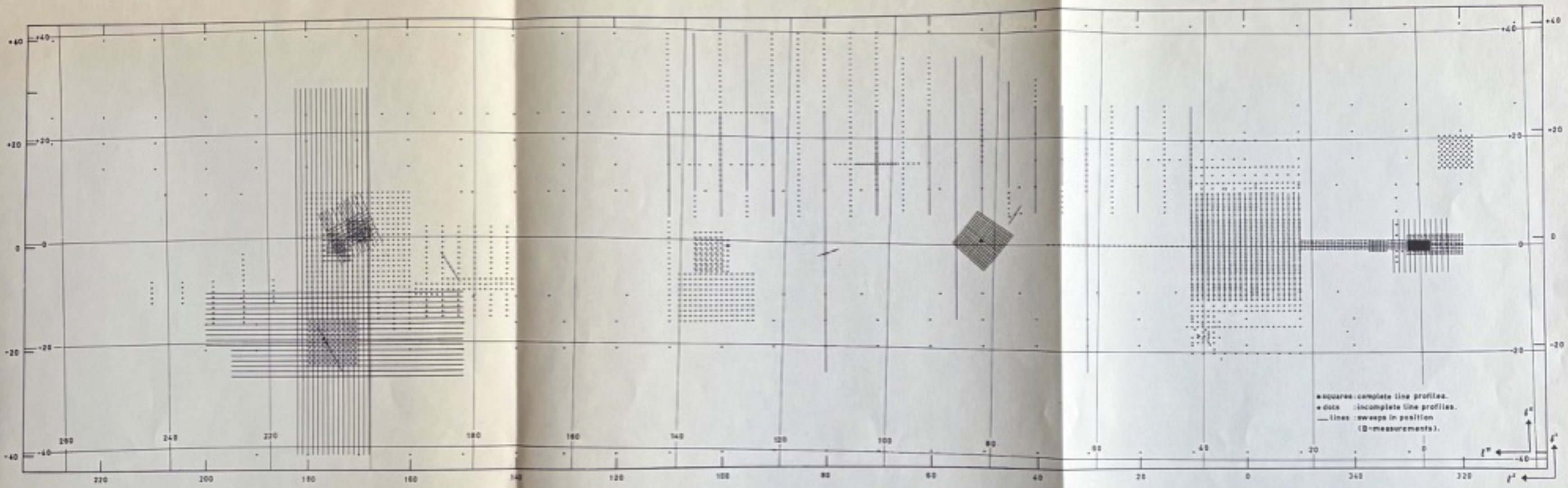

■ squares : complete line profiles.
• dots : incomplete line profiles.
— lines : sweeps in position (B-measurements).

Absorption profiles Cas A	09	CAM	A	E	350.39	350.39	+58.57	+58.57	0	0	- 145	+ 600	{2.5 5	5 8	2 2	2 2 }	2	1	feb-apr 58
			A	E	348.00	352.00	+58.60	+58.60	4.0	0	- 145	+ 600	5	8	2	2	2	1	feb-apr 58
			B_α	E	346.0	354.0	+58.60	+58.60	0.25	0	- 84	+ 325	10	8	1	1	42	1	feb-apr 58
Cyg A			A	E	299.51	299.51	+40.61	+40.61	0	0	- 310	+ 720	{2.5 5	5 8	2 2	2 2 }	2	1	feb-apr 58
			A	E	298.70	300.30	+39.82	+41.42	1.60	1.60	- 310	+ 720	5	8	2	2	2	1	feb-apr 58
			B_α	E	297.0	302.4	+40.61	+40.61	0.25	0	- 300	+ 750	10	8	1	1	106	1	feb-apr 58
Tau A			A	E	83.00	83.00	+21.99	+21.99	0	0	- 200	+ 200	{2.5 5	5 8	2 2	2 2 }	2	1	feb-apr 58
			A	E	82.00	84.00	+22.08	+22.08	2.0	0	- 200	+ 200	5	8	2	2	2	1	feb-apr 58
			B_α	E	79.5	86.5	+21.99	+21.99	0.25	0	- 200	+ 200	10	8	1	1	41	1	feb-apr 58

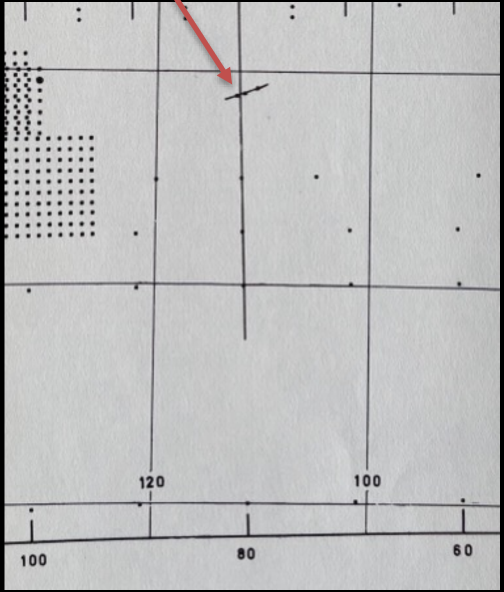

PAPER 69

21-CM HYDROGEN-LINE ABSORPTION IN THE SPECTRA OF DISCRETE SOURCES

C. A. MULLER
Radio Observatory, Dwingeloo, The Netherlands

This paper is a short survey of the results obtained with the Dwingeloo 25-meter radio telescope (beamwidth 0°56) and the 21-cm receiver on hydrogen-line absorption effects in the spectra of a number of strong point sources. Earlier work on this subject has been done by Hagen, Lilley, and McClain [1], and by Davies and Williams [2]. Some preliminary results of the first part of the present investigation were already published [3].

1. GENERAL METHOD

The hydrogen-line profile observed with a radio telescope pointing at a discrete source may be considered to consist of two parts: (1) The *emission profile* due to all neutral-hydrogen clouds in the antenna beam which would be measured in the absence of the source; this profile we shall call "the expected profile" following Hagen, Lilley, and McClain. (2) The *absorption profile* due to the absorption of the continuous radiation of the discrete source by hydrogen clouds lying between the source and the telescope; this profile we will call "the true absorption profile." Since usually the width of the source is much smaller than the beamwidth of the telescope the expected profile is mainly determined by clouds or parts of clouds within the antenna beam but not in front of the source; while the source's possible absorption of hydrogen radiation from clouds behind it can be neglected.

Assuming a uniform hydrogen distribution over the solid angle of the source, we may write for the observed profile:

$$T_{obs}(\nu) = T_{exp}(\nu) - T_a(1 - e^{-\tau(\nu)}) ,$$

where T_a is the observed antenna temperature due to the continuous radiation from the source outside the hydrogen-line frequencies, and $\tau(\nu)$ is the optical depth of the neutral hydrogen in front of the source. The true absorption spectrum is given by the term $T_a e^{-\tau(\nu)}$, while the term $-T_a$ is introduced by the comparison method used in the receiver.

To obtain the true absorption profile and from it the optical depth of the hydrogen clouds we must find the expected profile and subtract it from the observed profile. Though it is impossible to determine the expected profile, in principle we can obtain a good approximation from measuring the hydrogen radiation in the immediate neighborhood of the source. In earlier work this was done by using the mean of a number of profiles taken around the source. We have tried to improve on this method by using

constant-declination or constant-galactic-latitude scans [3] across the source at a large number of frequencies to derive the expected profile. The main reason for using this method was that in several cases large differences in slope of the intensity-versus-declination (or galactic-latitude) curves were found to occur on both sides of the absorption dip in the curve, which would lead to an incorrect expected profile when taking the simple mean of profiles on both sides of the source. Constant-declination scans were used in the cases of Cassiopeia A, Taurus A, and Orion A, while for Cygnus A and Sagittarius A constant-galactic-latitude scans were chosen. In the case of Virgo A, comparison measurements on a number of surrounding points were made in the same way as the observations for M 31 were made by van de Hulst, Raimond, and van Woerden [4].

Figs. 1 to 5 give the measured profile and the expected profile, together with the true absorption profile derived from these two by subtraction. All the observed profiles were taken with a receiver bandwidth of 5 kc/s, corresponding to 1 km/second, while the scans and comparison profile were taken with a bandwidth of 10 kc/s, because the expected profile does not show the fine structure of the absorption profile and thus could be measured with a somewhat wider beamwidth with the advantage of smaller noise fluctuations. The r.m.s. noise fluctuation on the mean observed profile is about 1 °K and slightly larger for the expected profile in most cases.

2. INDIVIDUAL SOURCES

Cassiopeia A: A profile taken with a 10-kc/s beamwidth has already been published [3]. New 5-kc/s observations confirm the earlier results and reveal one more component on the low-frequency slope of the strong line at −38 km/second. A total of eight components have now been found: four due to absorption in the Orion arm and four due to the Perseus arm. The absorption in the latter arm is stronger than in the first, with optical depths to 3 or 4, while in the Orion arm the absorption is less than 2. This is the only available case of absorption in the Perseus arm. Of interest are the three components with optical depth less than 0.1 in the Orion arm.

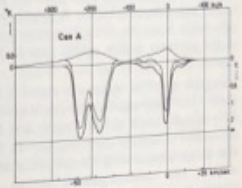

FIG. 1. Absorption profile of Cas A. The temperature indications in Figs. 1 through 5 are antenna temperatures, and are smaller than the brightness temperatures used in other Dutch papers by approximately 30 per cent. *Upper curve*: expected profile; *middle curve*: observed profile; *lower curve*: true absorption profile.

A comparison with theoretical gaussian profiles generally gives a very good agreement, though the tails extend somewhat farther out than a gaussian profile. The same effect of a slightly wider tail was found in the spectra of other sources where a separation of the spectra into individual components made the assump-

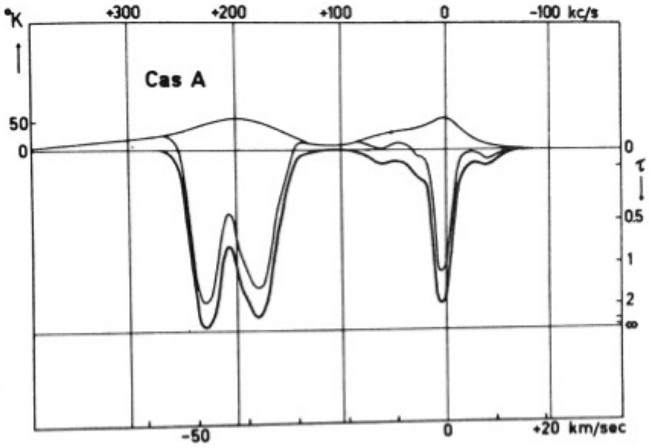

FIG. 1. Absorption profile of Cas A. The temperature indications in Figs. 1 through 5 are antenna temperatures, and are smaller than the brightness temperatures used in other Dutch papers by approximately 30 per cent. *Upper curve*: expected profile; *middle curve*: observed profile; *lower curve*: true absorption profile.

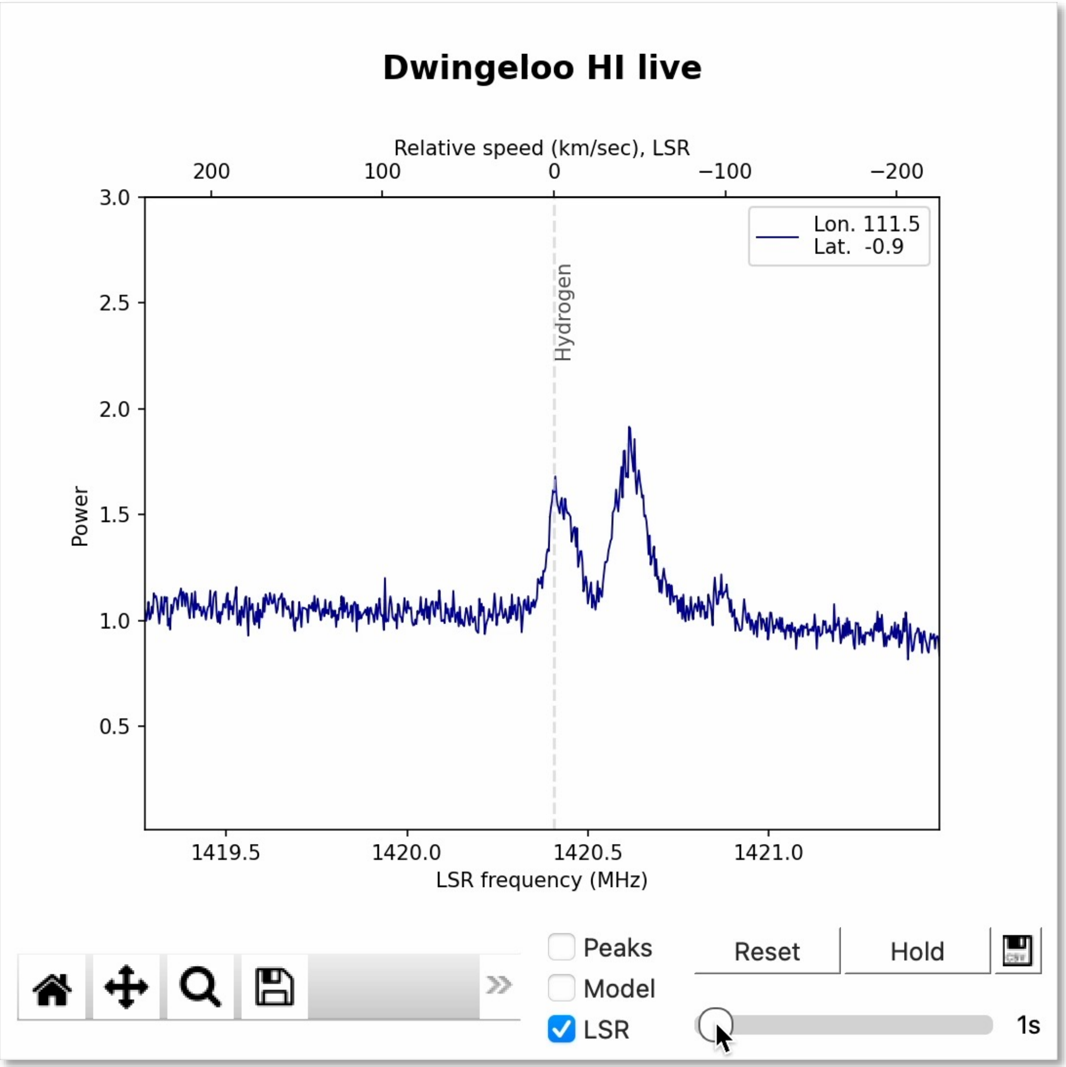

No. 4909 November 30, 1963 NATURE 829

RADIO OBSERVATIONS OF OH IN THE INTERSTELLAR MEDIUM

By Dr. S. WEINREB
Lincoln Laboratory, Massachusetts Institute of Technology
Prof. A. H. BARRETT
Research Laboratory of Electronics, Massachusetts Institute of Technology, Cambridge, Mass.
AND
Dr. M. L. MEEKS and J. C. HENRY
Lincoln Laboratory, Massachusetts Institute of Technology, Lexington, Mass.

IN this article we wish to report the detection of 18-cm absorption lines of the hydroxyl (OH) radical in the radio absorption spectrum of Cassiopeia *A*, thereby providing positive evidence for the existence of OH in the interstellar medium. The microwave transitions of OH in the ground-state, $^2\pi_{3/2}$, $J = 3/2$, arise from two

Λ-type doublet-levels, each of which is
interactions with the hydrogen nucle
transitions result. The two strongest
previously measured in the laborator
0·03 Mc/s ($F = 2 \rightarrow 2$) and 1,665·
($F = 1 \rightarrow 1$) with relative intensities of

(2) The OH absorption spectra at both frequencies show general agreement with the H absorption spectra.

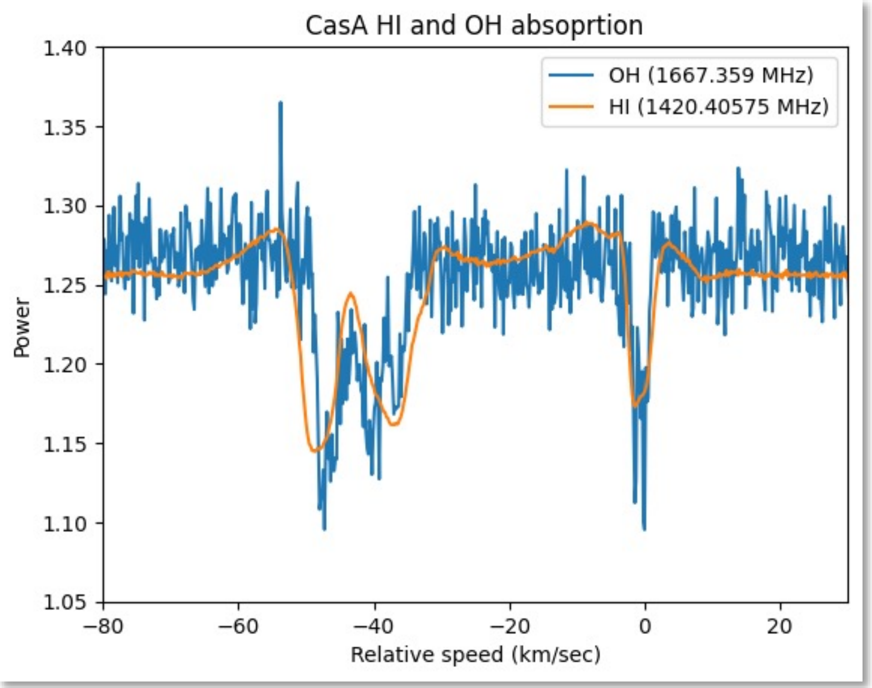

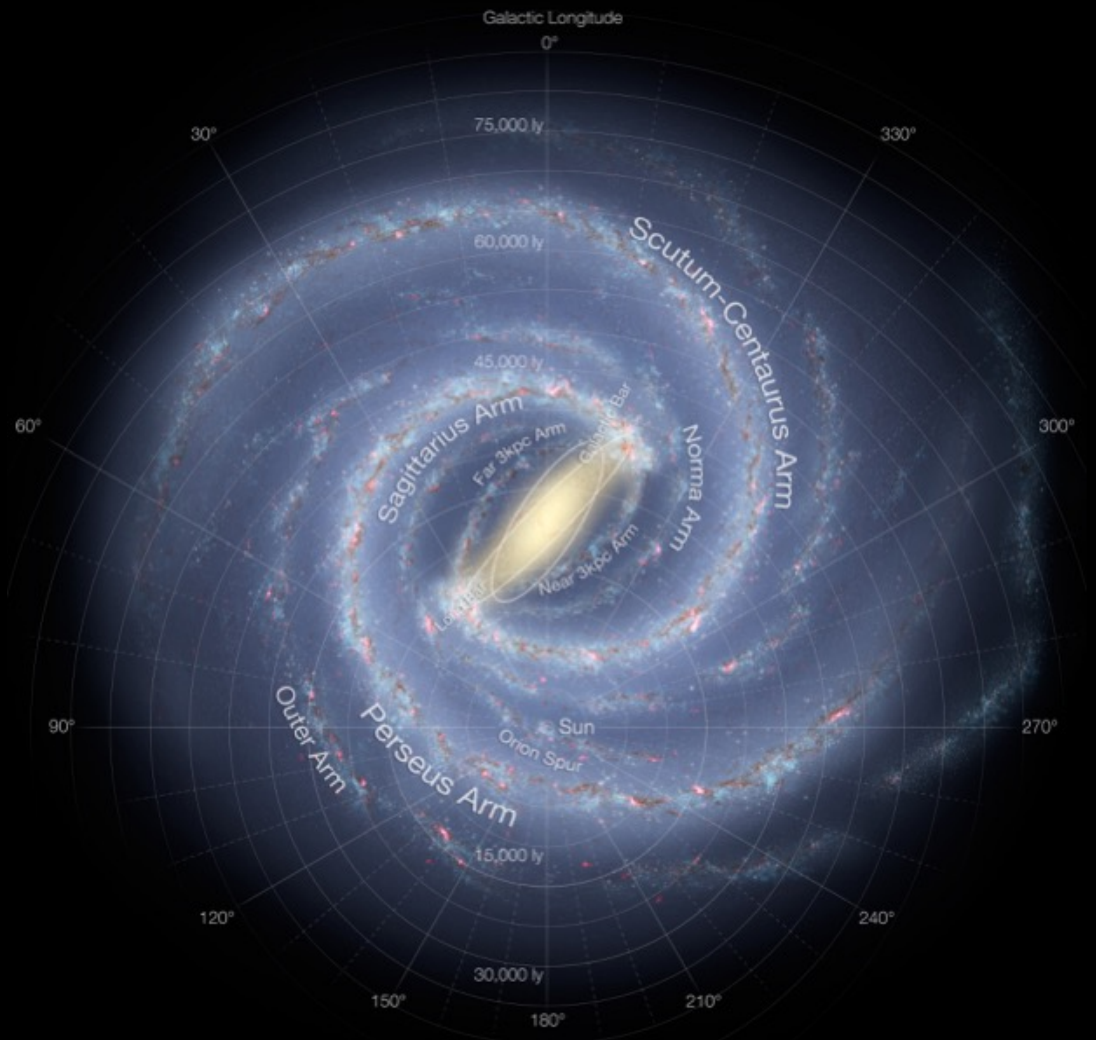

Galactic Longitude
0°
30°
330°
75,000 ly
60,000 ly
45,000 ly
Scutum-Centaurus Arm
Sagittarius Arm
Far 3kpc Arm
Norma Arm
60°
300°
Near 3kpc Arm
90°
270°
Sun
Orion Spur
Outer Arm
Perseus Arm
15,000 ly
30,000 ly
120°
240°
150°
210°
180°

ASTRONOMIE. — *Expansion d'une structure spirale dans le noyau du Système Galactique, et position de la radiosource* Sagittarius *A*. Note (*) de MM. **Hugo van Woerden**, **Willem Rougoor** et **Jan Oort**.

Au cours d'une étude de la radiation 21 cm de l'hydrogène on a trouvé, dans la partie centrale du Système Galactique ($R < 2$ kpc), des bras spiraux qui s'éloignent du centre avec des vitesses de 50 à 100 km/s. Un de ces bras cause une forte absorption de la raie 21 cm dans la source *Sagittarius A*. Ceci montre qu'en toute probabilité cette source est située au centre de notre Galaxie.

Un des premiers points du programme du nouveau radiotélescope de 25 m à Dwingeloo, Pays-Bas, est une étude de la radiation 21 cm de l'hydrogène issue de la partie centrale de la Galaxie.

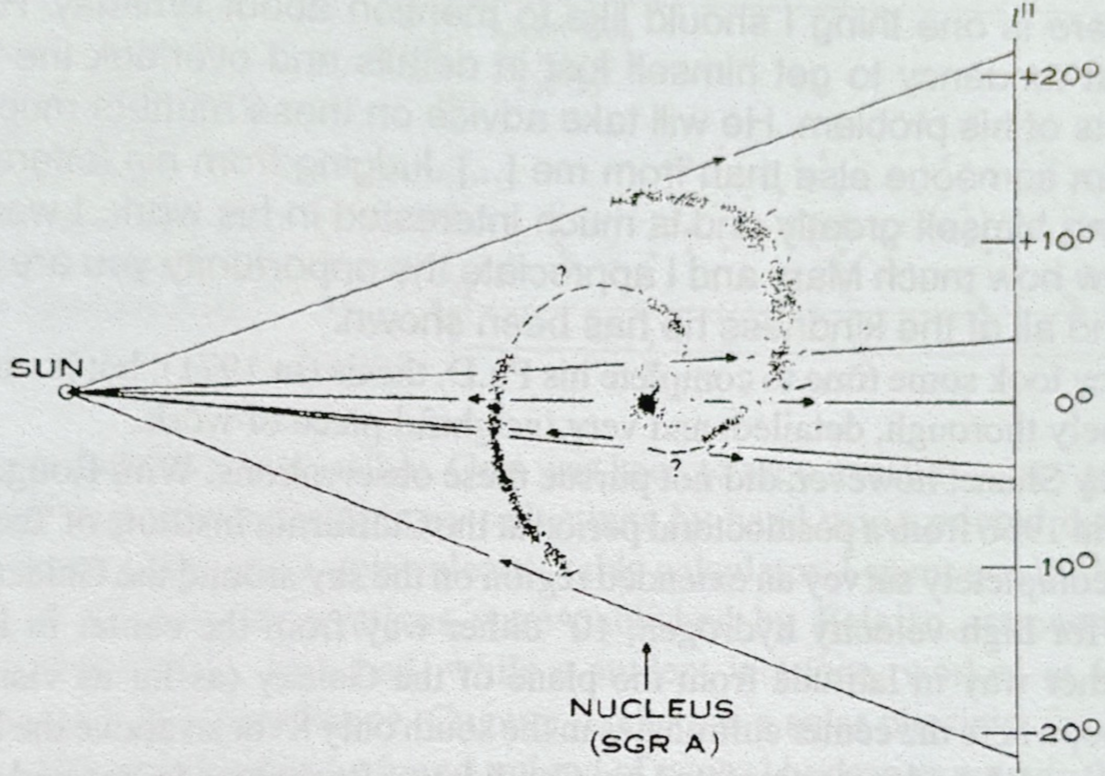

Fig. 13.14 Oort's schematic drawing of the neutral hydrogen in the central part of the Galaxy that he used in various publications and presentations. The 3-kpc arm on the left is seen in absorption and moves towards the Sun at 53 km/s in front of the central radio source Sagittarius A (Sgr A), while on the opposite side there is no absorption from the arm moving at 135 km/s. From the Oort Archives

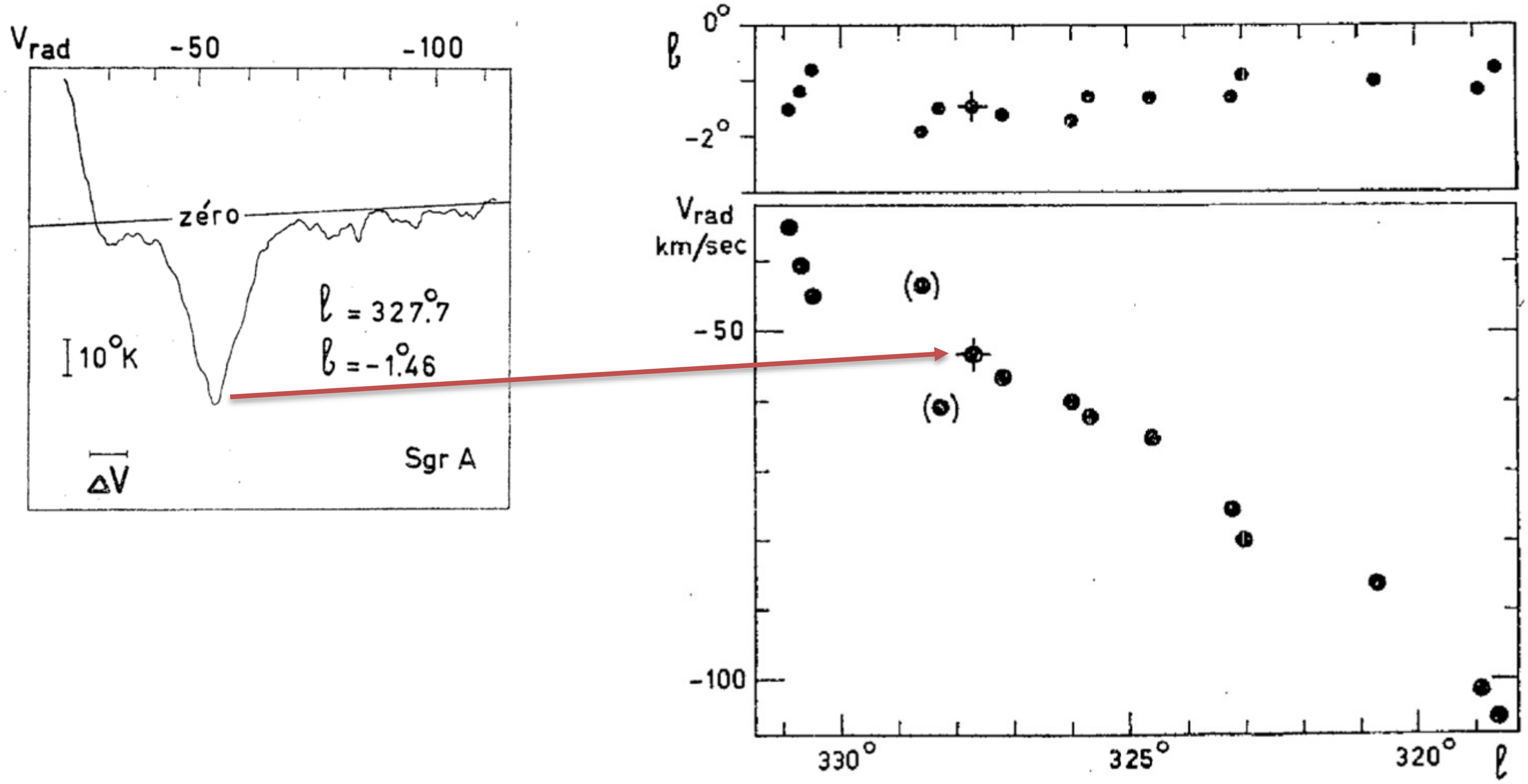
V rad
-50
-100
zéro
ℓ = 327°.7
b = -1°.46
10°K
ΔV
Sgr A
b
0°
-2°
V rad
km/sec
-50
-100
330°
325°
320°
ℓ

Fig. 3.

3 kpc Arm, 1957/2025

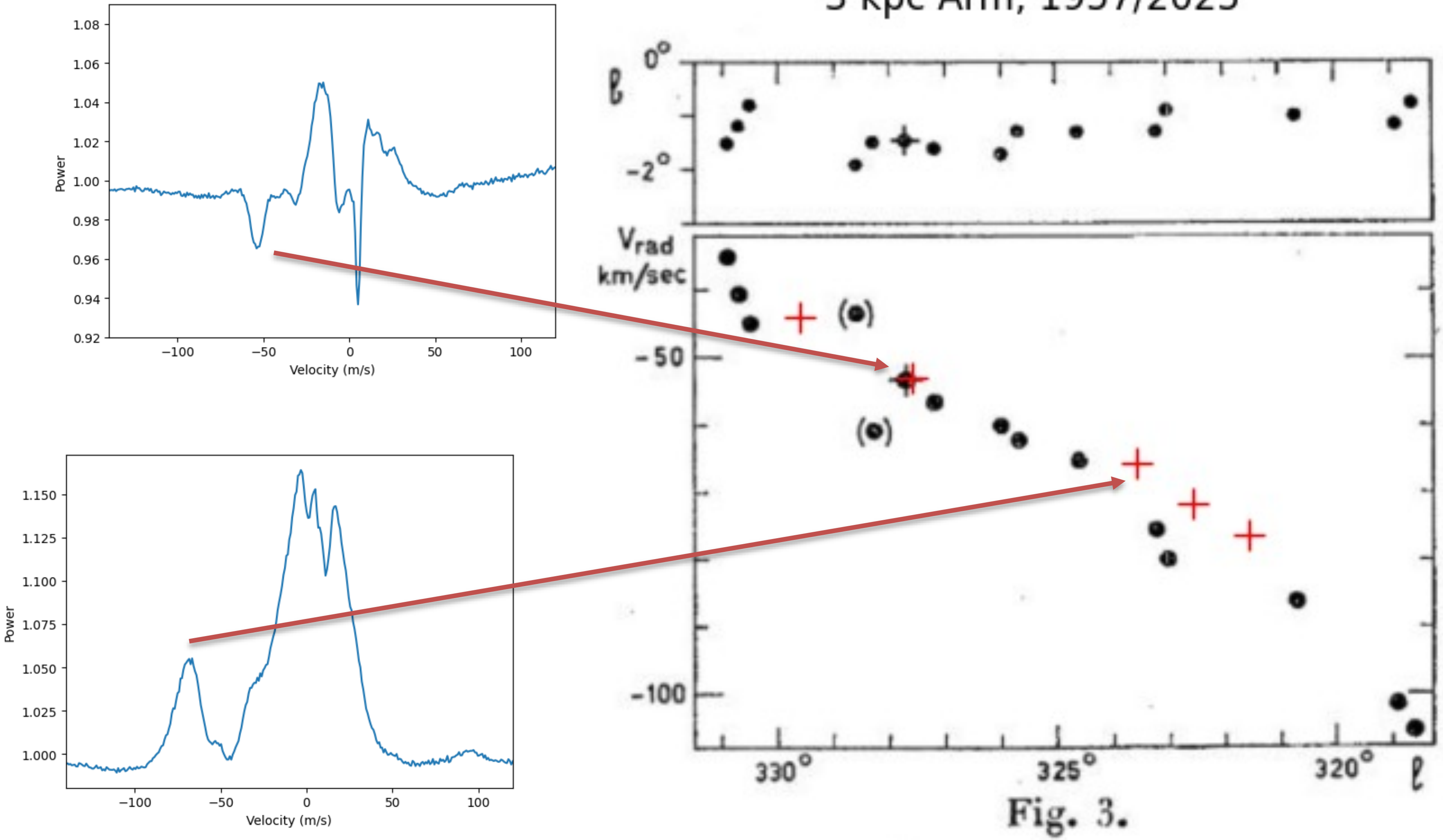

Fig. 3.

1	2	3	4	5	6			7		8	9	10		11
extragalactic nebula	program number	investi-gator	α	δ	distance from centre of nebula			limits of velocity interval		spacing in velocity	number of meas. per profile	comparison fields		dates
						in direction of								
					abs.	major axis	minor axis	lower	upper			more than one used for velocities	total number	
			°	°										
NGC 224 (M 31)	21	HCvdH	12.16	+ 43.										
		ER	11.76	+ 42.										
		HvW	11.54	+ 42.										
			11.33	+ 42.										
			11.12	+ 41.										
			10.71	+ 41.										
			10.50	+ 41.										
			10.30	+ 41.										
			10.09	+ 41.										
			9.89	+ 40.										
			9.69	+ 40.										
			9.49	+ 40.										
			9.28	+ 40.										
			9.08	+ 40.										
			8.89	+ 39.										
			8.69	+ 39.										
			8.50	+ 39.										
			8.30	+ 39.										
			8.11	+ 39.										
			7.92	+ 38.										

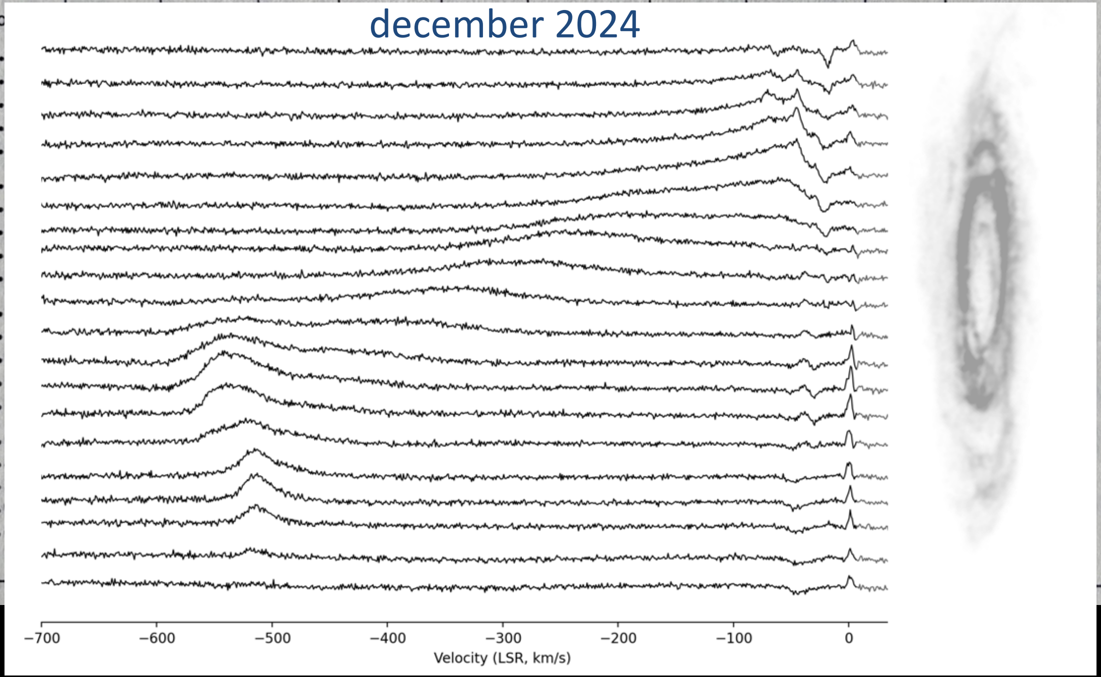

Hydrogen spectral emissions

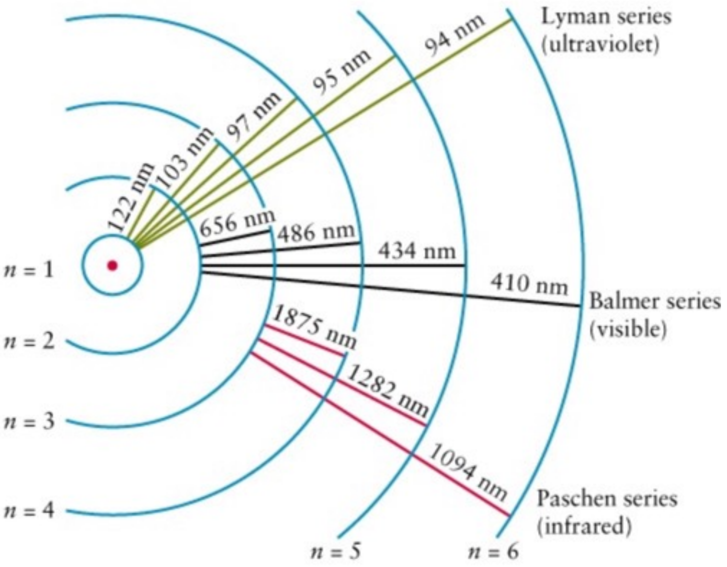

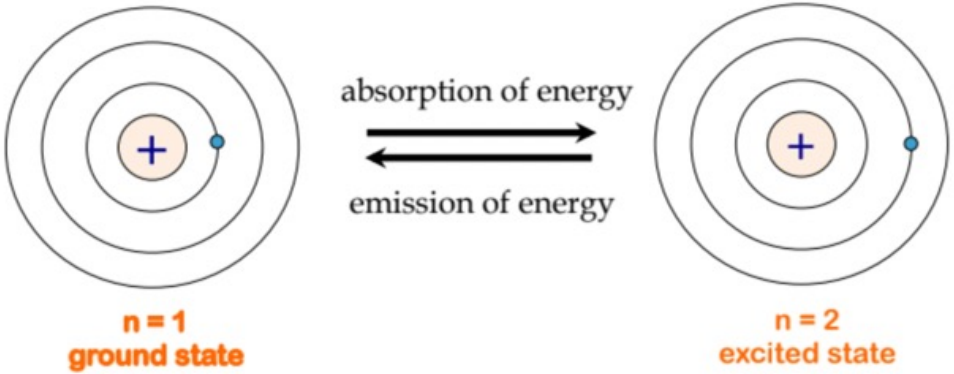

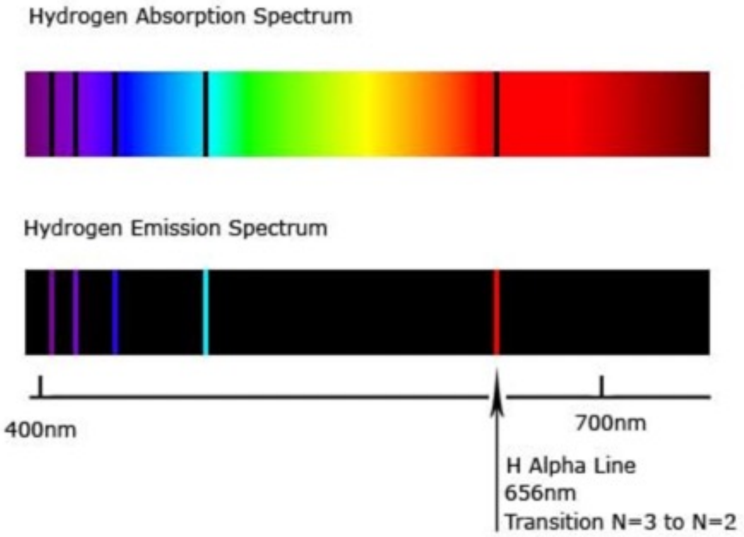

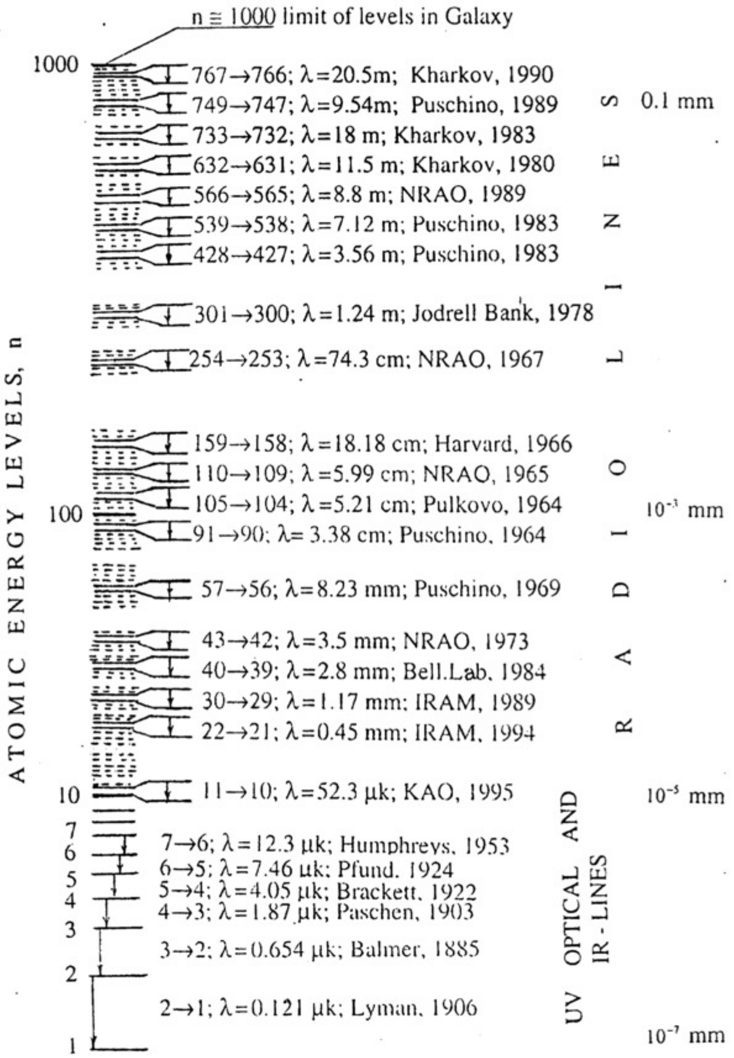
n ≅ 1000 limit of levels in Galaxy
1000
767→766; λ=20.5m; Kharkov, 1990
749→747; λ=9.54m; Puschino, 1989
733→732; λ=18 m; Kharkov, 1983
632→631; λ=11.5 m; Kharkov, 1980
566→565; λ=8.8 m; NRAO, 1989
539→538; λ=7.12 m; Puschino, 1983
428→427; λ=3.56 m; Puschino, 1983
301→300; λ=1.24 m; Jodrell Bank, 1978
254→253; λ=74.3 cm; NRAO, 1967
159→158; λ=18.18 cm; Harvard, 1966
110→109; λ=5.99 cm; NRAO, 1965
105→104; λ=5.21 cm; Pulkovo, 1964
100
91→90; λ= 3.38 cm; Puschino, 1964
57→56; λ=8.23 mm; Puschino, 1969
43→42; λ=3.5 mm; NRAO, 1973
40→39; λ=2.8 mm; Bell.Lab, 1984
30→29; λ=1.17 mm; IRAM, 1989
22→21; λ=0.45 mm; IRAM, 1994
10
11→10; λ=52.3 μk; KAO, 1995
7
6
5
4
3
2
1
7→6; λ=12.3 μk; Humphreys, 1953
6→5; λ=7.46 μk; Pfund, 1924
5→4; λ=4.05 μk; Brackett, 1922
4→3; λ=1.87 μk; Paschen, 1903
3→2; λ=0.654 μk; Balmer, 1885
2→1; λ=0.121 μk; Lyman, 1906
ATOMIC ENERGY LEVELS, n
RADIO LINES
UV OPTICAL AND IR - LINES
0.1 mm
10⁻³ mm
10⁻⁵ mm
10⁻⁷ mm

Omega Nebula (M17/W38)

1966

1968, *Bull. Astr. Inst. Netherlands* **19** 460–468;
Communication from the Netherlands Foundation for Radio Astronomy and the Kapteyn Astronomical Laboratory at Groningen

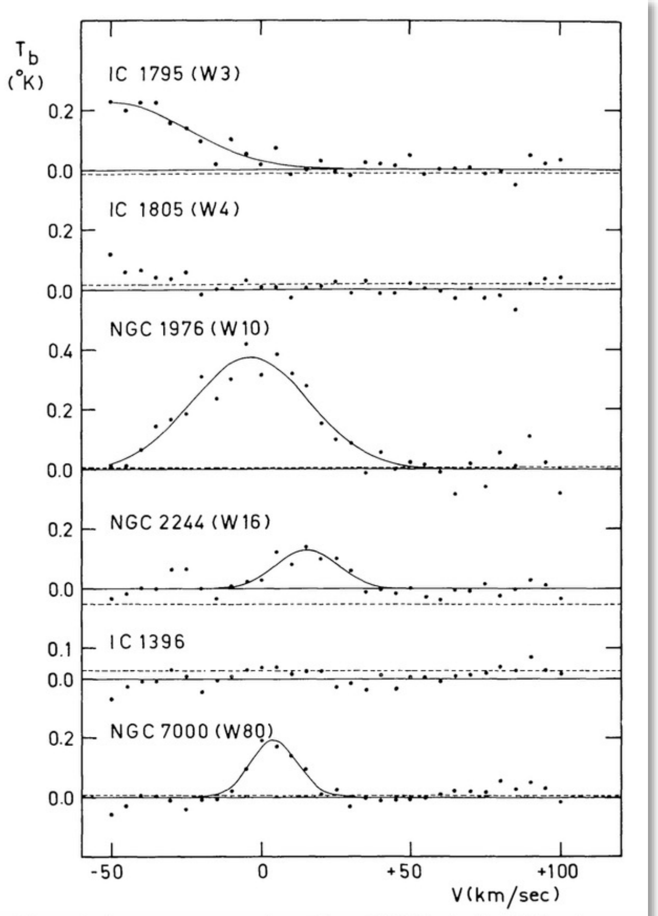

Figure 2. Average measured profiles of H166α in six H II regions.

OBSERVATIONS OF THE HYDROGEN RECOMBINATION LINE H166α IN GALACTIC H II REGIONS

J. A. DE BOER, A. C. HIN, U. J. SCHWARZ and H. VAN WOERDEN

Received 2 February 1968

2025

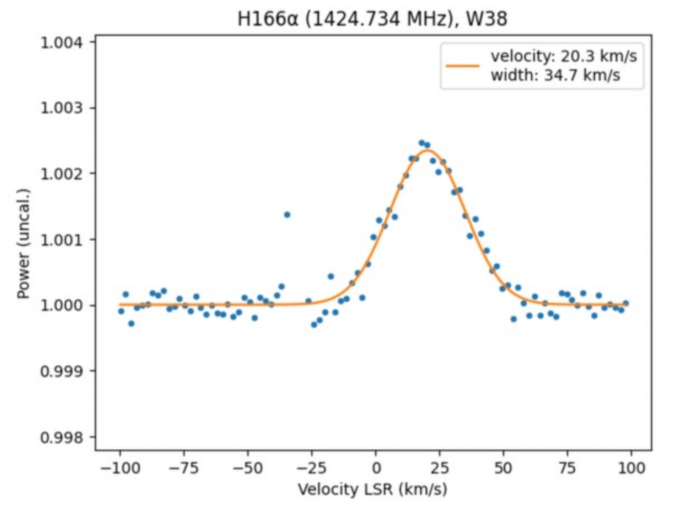

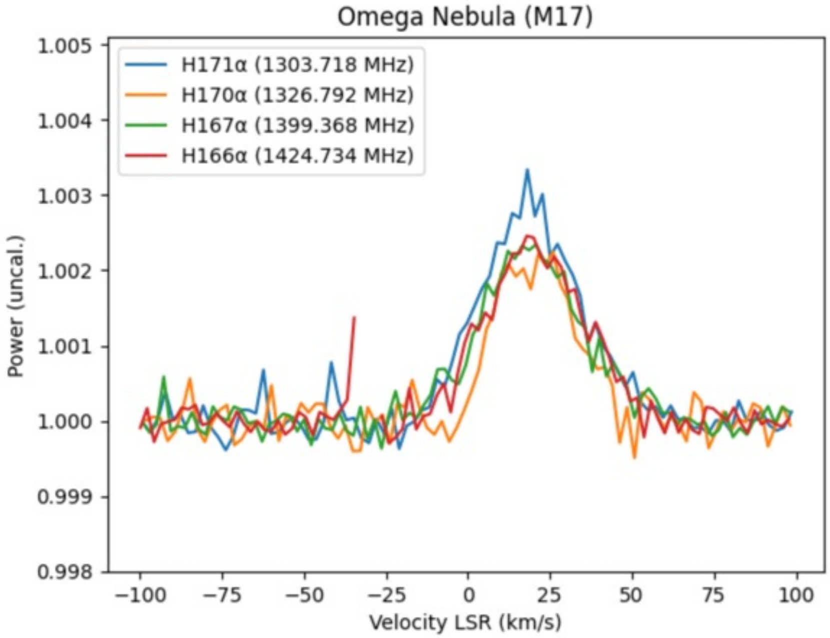
Omega Nebula (M17)
H171α (1303.718 MHz)
H170α (1326.792 MHz)
H167α (1399.368 MHz)
H166α (1424.734 MHz)
Power (uncal.)
1.005
1.004
1.003
1.002
1.001
1.000
0.999
0.998
−100
−75
−50
−25
0
25
50
75
100
Velocity LSR (km/s)

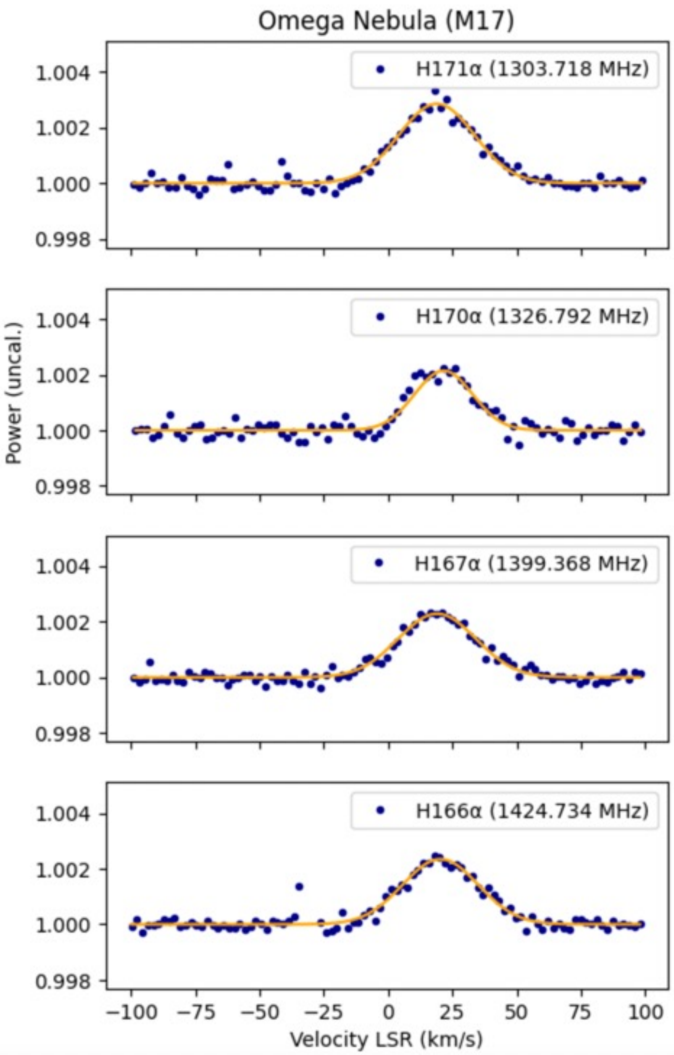
Omega Nebula (M17)
H171α (1303.718 MHz)
H170α (1326.792 MHz)
H167α (1399.368 MHz)
H166α (1424.734 MHz)
Power (uncal.)
1.004
1.002
1.000
0.998
−100
−75
−50
−25
0
25
50
75
100
Velocity LSR (km/s)

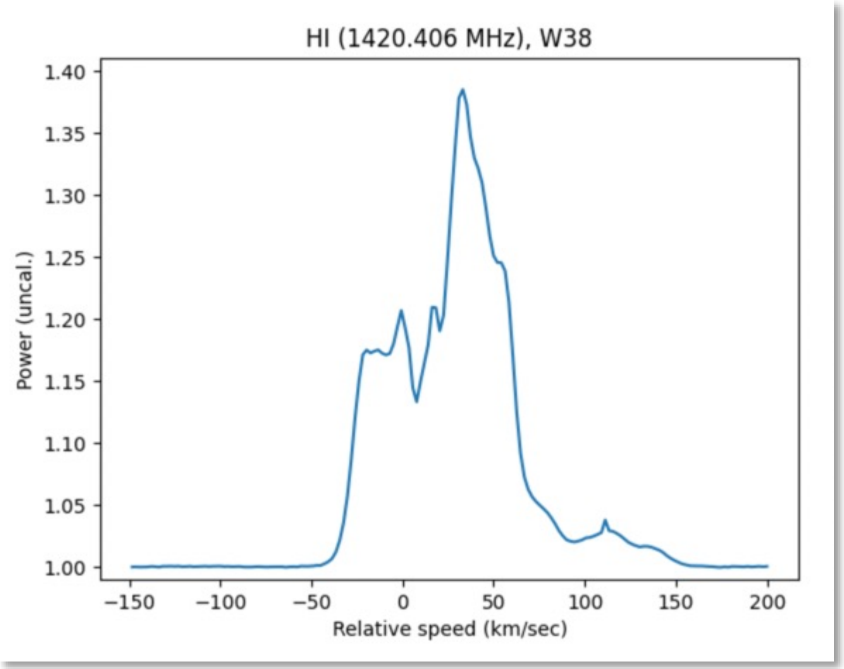
HI (1420.406 MHz), W38
Power (uncal.)
1.40
1.35
1.30
1.25
1.20
1.15
1.10
1.05
1.00
−150
−100
−50
0
50
100
150
200
Relative speed (km/sec)

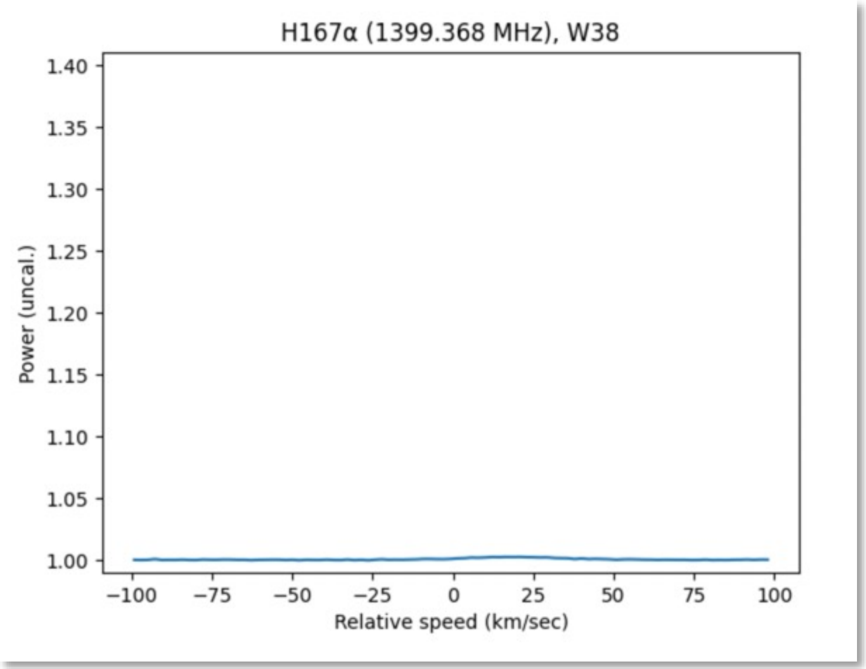
H167α (1399.368 MHz), W38
Power (uncal.)
1.40
1.35
1.30
1.25
1.20
1.15
1.10
1.05
1.00
−100
−75
−50
−25
0
25
50
75
100
Relative speed (km/sec)

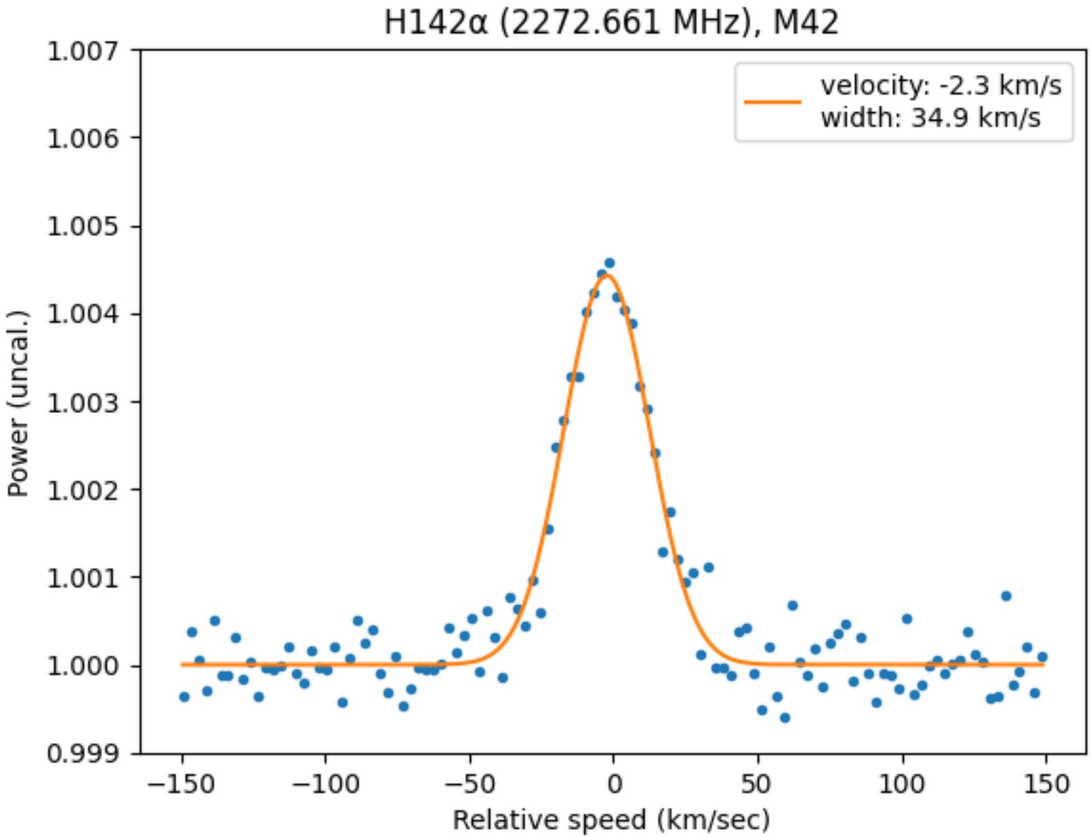

H142α (2272.661 MHz), M42
velocity: -2.3 km/s
width: 34.9 km/s
Power (uncal.)
1.007
1.006
1.005
1.004
1.003
1.002
1.001
1.000
0.999
−150
−100
−50
0
50
100
150
Relative speed (km/sec)

https://www.astro.uni-bonn.de/hisurvey/euhou/LABprofile/

HI Profile Search

Select Position		
Coordinate system		Galactic coordinates (l, b)
Position	RA [h m s]/ l [°]	353
	DEC [±° ' "]/ b [°]	22
Effective beamsize FWHM [°]		10.00
Velocity Window for display	Minimum [km/s]	-50.00
	Maximum [km/s]	50.00
Search data		

Dwingeloo

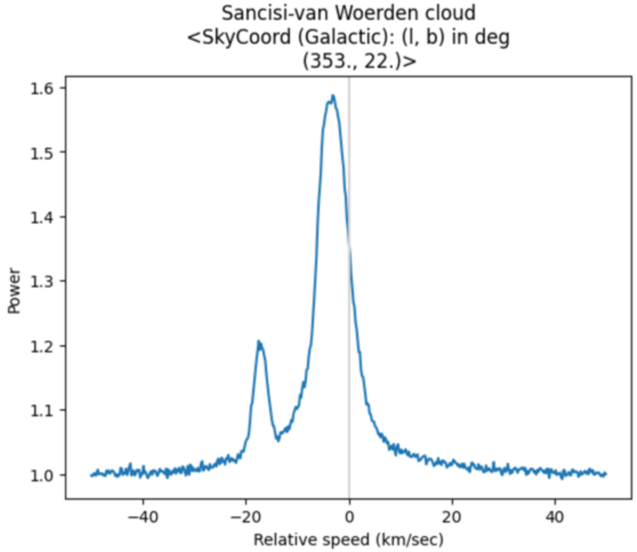

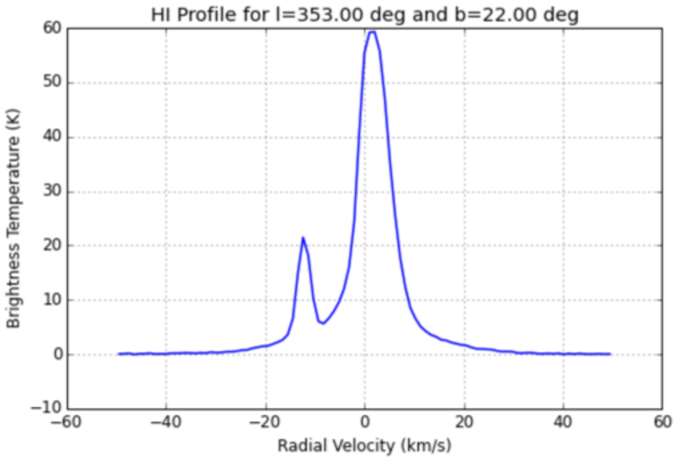

0.55°

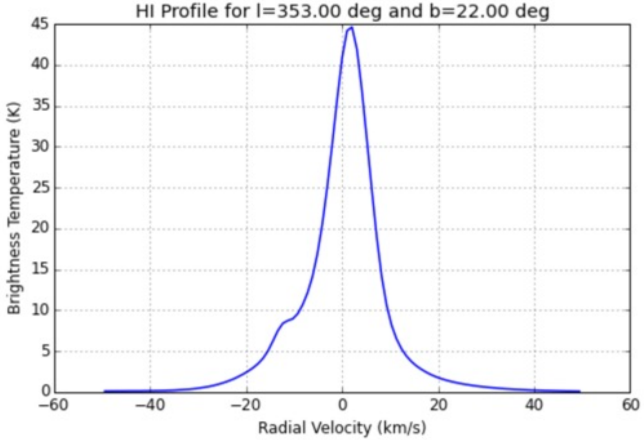

10°

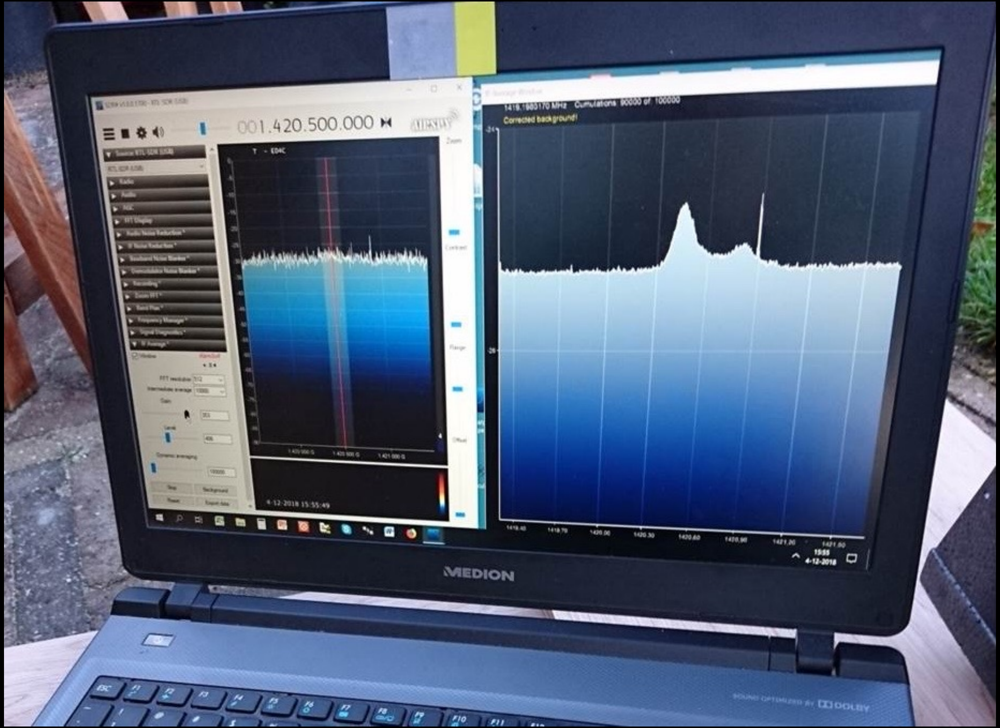
001.420.500.000
Corrected background!
MEDION

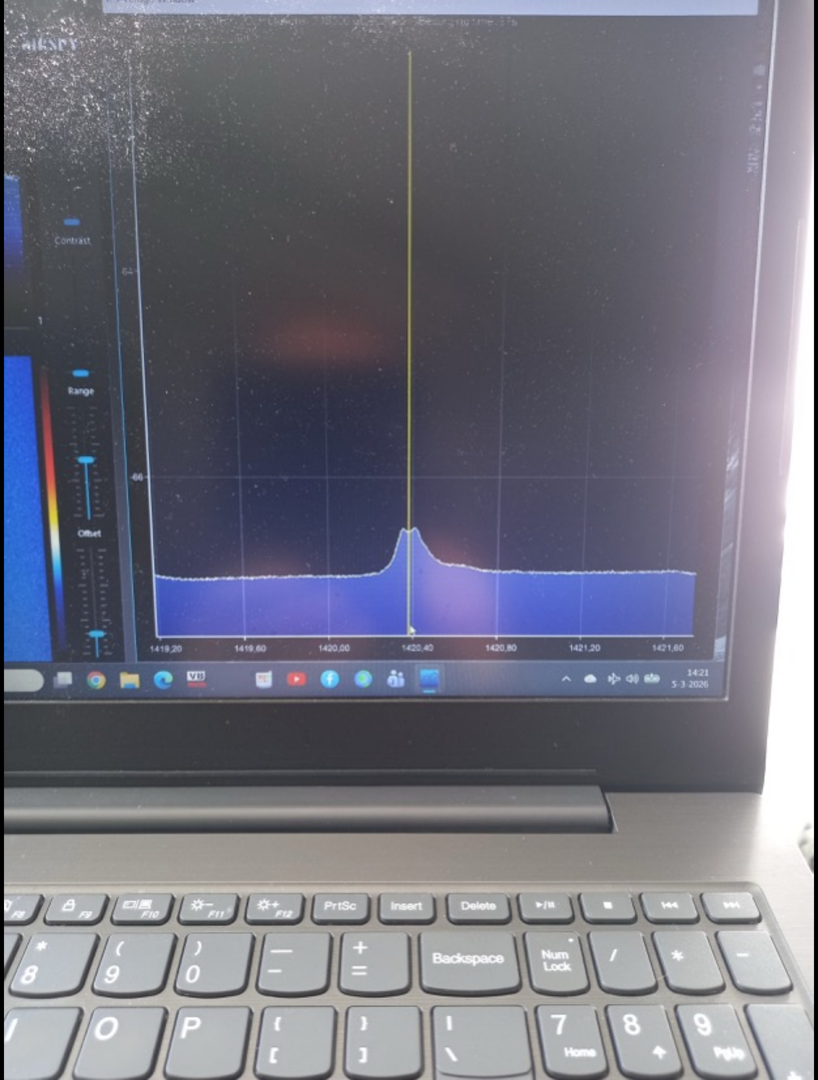
Contrast
Range
Offset
1419,20
1419,60
1420,00
1420,40
1420,80
1421,20
1421,60
14:21
5-3-2026
PrtSc
Insert
Delete
Backspace
Num Lock
Home

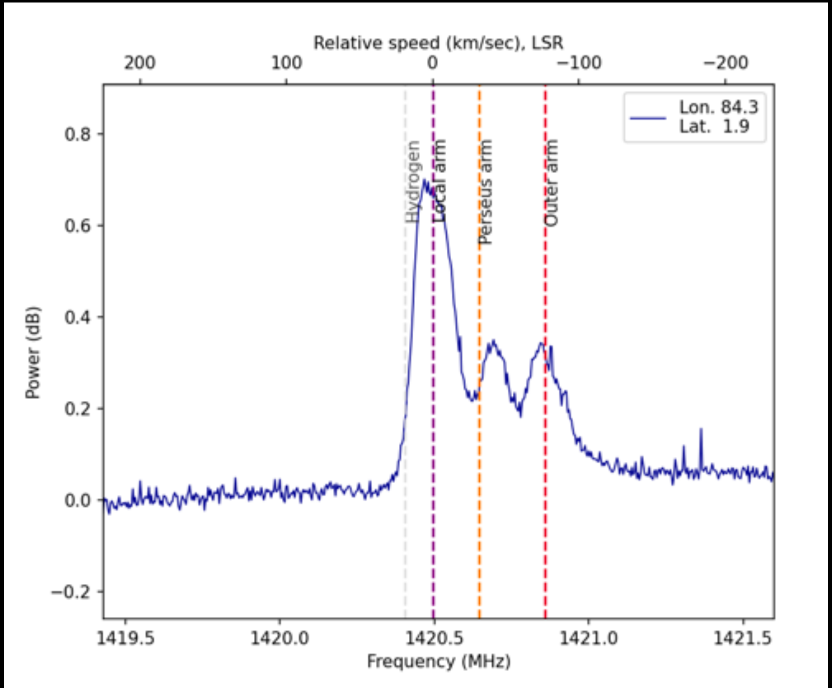
Relative speed (km/sec), LSR
200
100
0
−100
−200
Lon. 84.3
Lat. 1.9
Hydrogen
Local arm
Perseus arm
Outer arm
0.8
0.6
0.4
0.2
0.0
−0.2
Power (dB)
1419.5
1420.0
1420.5
1421.0
1421.5
Frequency (MHz)

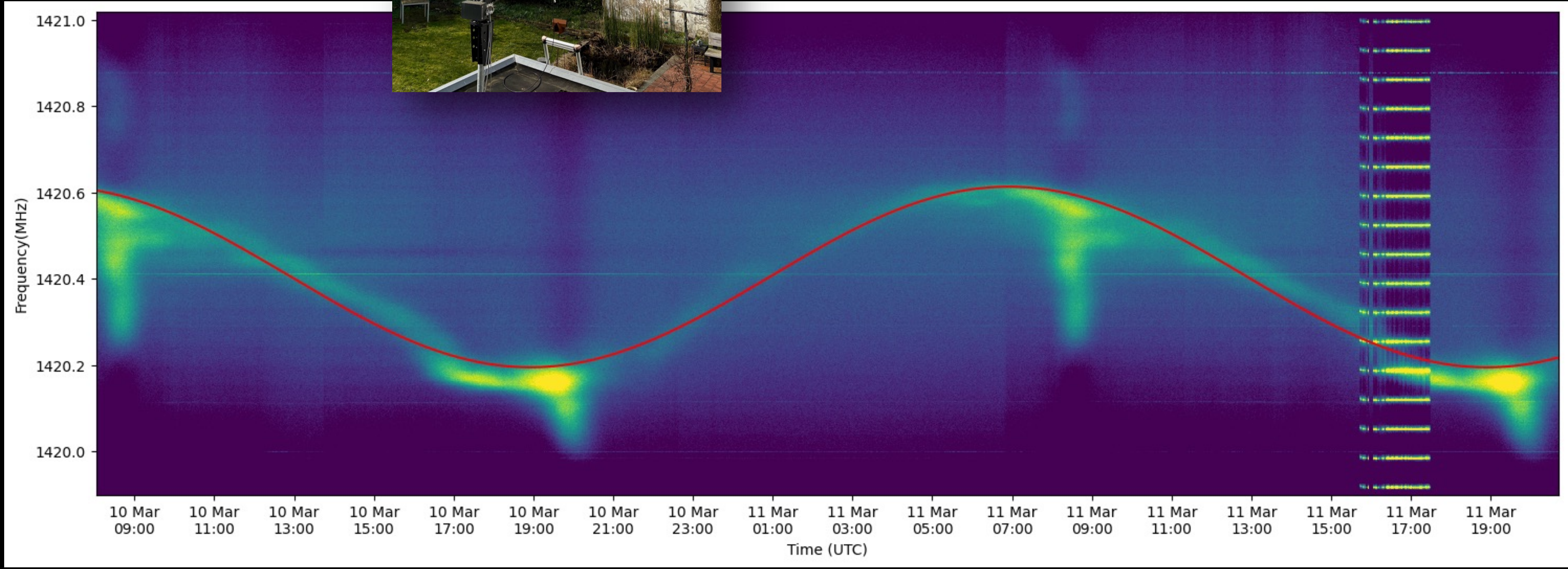

1421.0
1420.8
1420.6
1420.4
1420.2
1420.0
Frequency(MHz)
10 Mar 09:00
10 Mar 11:00
10 Mar 13:00
10 Mar 15:00
10 Mar 17:00
10 Mar 19:00
10 Mar 21:00
10 Mar 23:00
11 Mar 01:00
11 Mar 03:00
11 Mar 05:00
11 Mar 07:00
11 Mar 09:00
11 Mar 11:00
11 Mar 13:00
11 Mar 15:00
11 Mar 17:00
11 Mar 19:00
Time (UTC)

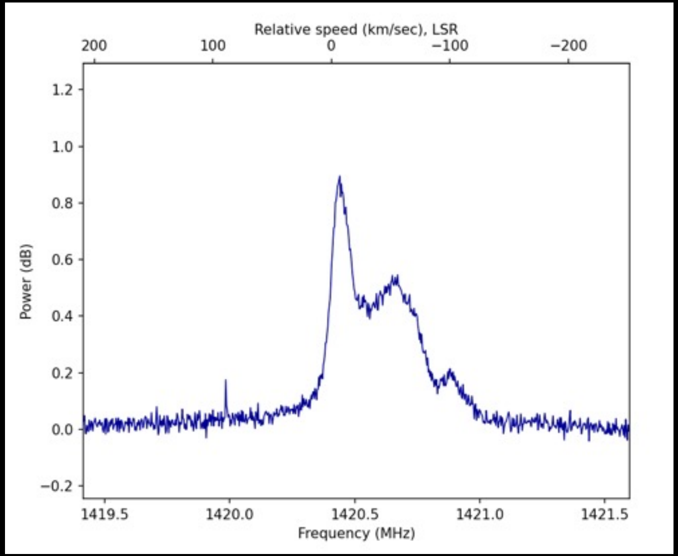

Relative speed (km/sec), LSR
200
100
0
−100
−200
1.2
1.0
0.8
0.6
0.4
0.2
0.0
−0.2
Power (dB)
1419.5
1420.0
1420.5
1421.0
1421.5
Frequency (MHz)

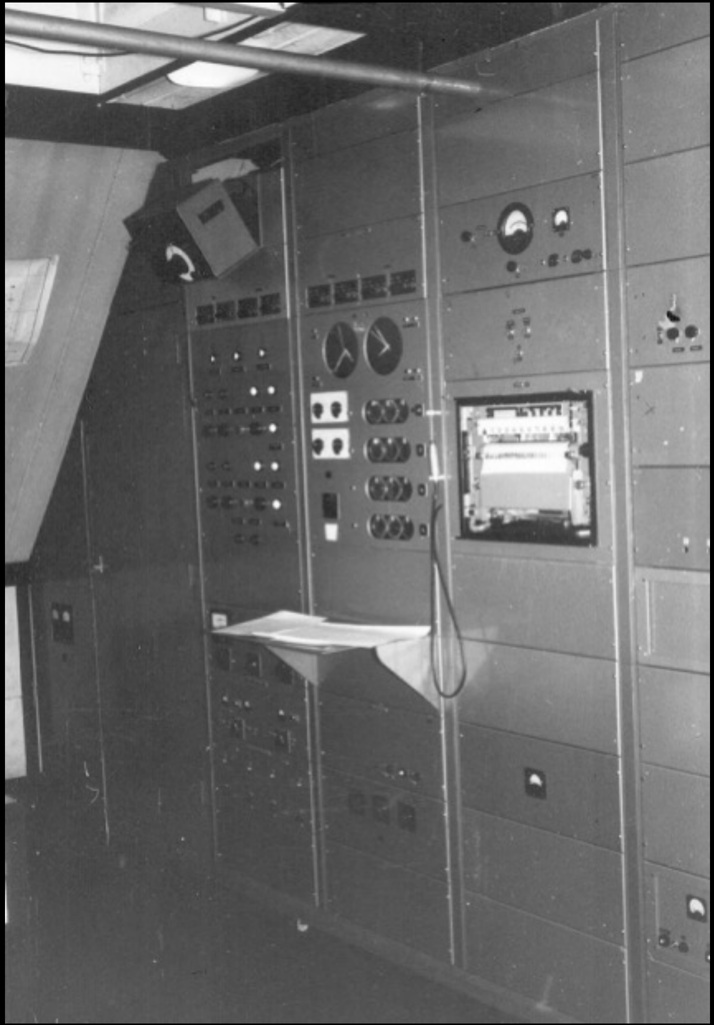

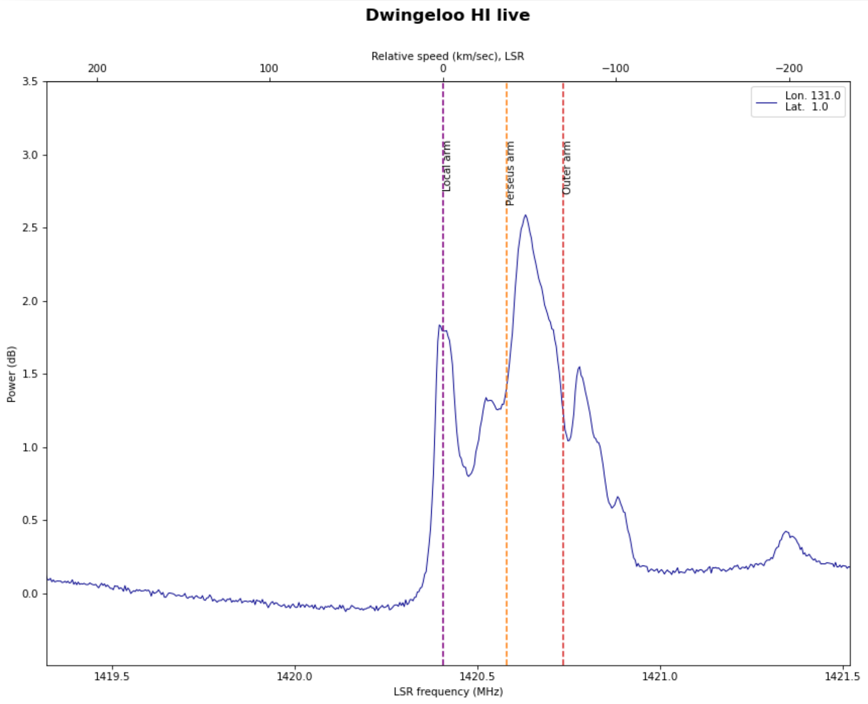
Dwingeloo HI live
Relative speed (km/sec), LSR
200
100
0
−100
−200
3.5
3.0
2.5
2.0
1.5
1.0
0.5
0.0
Power (dB)
Lon. 131.0
Lat. 1.0
Local arm
Perseus arm
Outer arm
1419.5
1420.0
1420.5
1421.0
1421.5
LSR frequency (MHz)

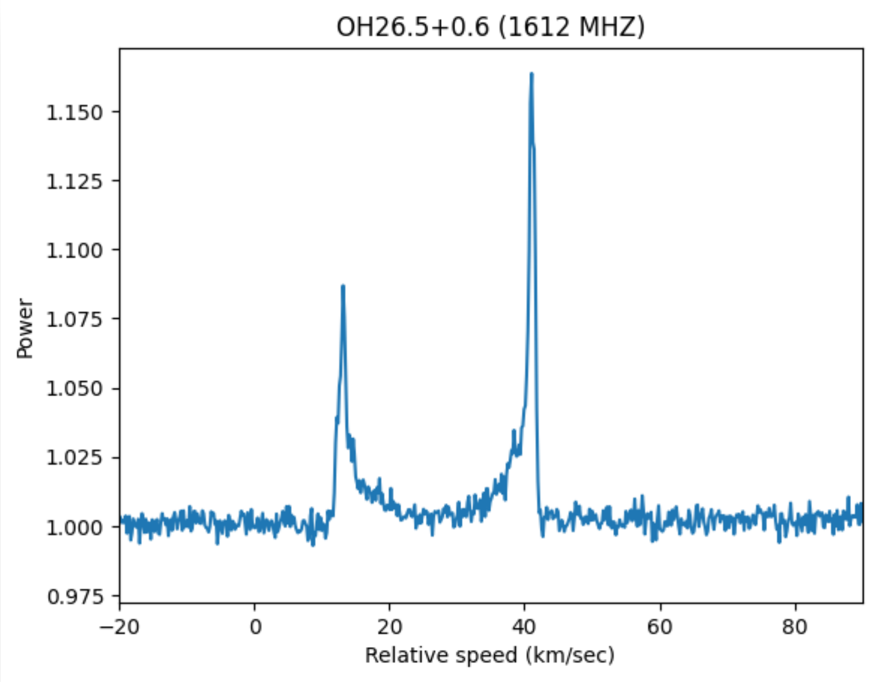
OH26.5+0.6 (1612 MHZ)
1.150
1.125
1.100
1.075
1.050
1.025
1.000
0.975
Power
−20
0
20
40
60
80
Relative speed (km/sec)

References

- https://github.com/tftelkamp/vrt-iq-tools
- https://gitlab.camras.nl/thomas/hi-demo-gui

- https://www.camras.nl/blog/2021/met-de-21-cm-waterstoflijn-van-kootwijk-naar-dwingeloo/

- https://www.astro.uni-bonn.de/hisurvey/euhou/LABprofile/index.php

- https://www.astropeiler.de/en/beobachtungen-der-21-cm-linie-mit-einfachen-mitteln/


CAMRAS
DWINGELOO TELESCOOP

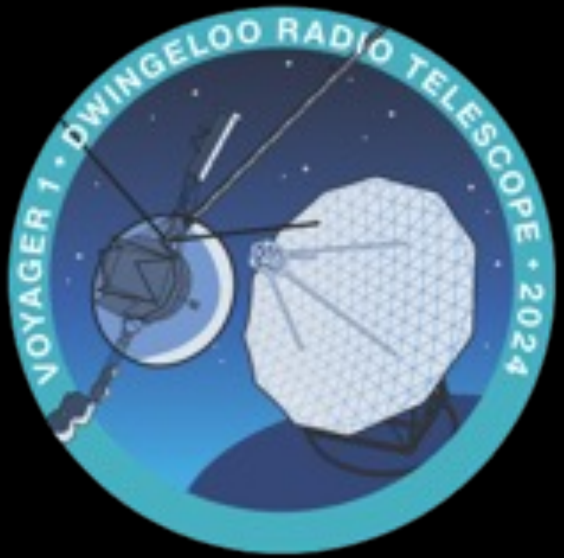
VOYAGER 1 • DWINGELOO RADIO TELESCOPE • 2024